NASA CONTRACTOR REPORT

NASA CR-1245

FLOW IN A TWO-DIMENSIONAL CHANNEL WITH A RECTANGULAR CAVITY

by Unmeel B. Mehta and Zalman Lavan

Prepared by
ILLINOIS INSTITUTE OF TECHNOLOGY
Chicago, Ill.
for Lewis Research Center

NATIONAL AERONAUTICS AND SPACE ADMINISTRATION • WASHINGTON, D. C. • JANUARY 1969

FLOW IN A TWO-DIMENSIONAL CHANNEL WITH A RECTANGULAR CAVITY

By Unmeel B. Mehta and Zalman Lavan

Prepared under Grants No. NGR 14-004-028 and NsG 694 by
ILLINOIS INSTITUTE OF TECHNOLOGY
Chicago, Ill.

for Lewis Research Center

NATIONAL AERONAUTICS AND SPACE ADMINISTRATION

For sale by the Clearinghouse for Federal Scientific and Technical Information
Springfield, Virginia 22151 – CFSTI price $3.00

FOREWORD

Research related to flow over aerodynamic bodies and to advanced nuclear propulsion is described herein. This work was performed under NASA Grants NGR 14-004-028 and NsG 694, with Mr. Maynard F. Taylor, Nuclear Systems Division, NASA Lewis Research Center as Technical Manager. A part of this work was also supported by the U.S. Air Force under contract AF-AFOSR 1081-66.

ABSTRACT

The steady-state flow characteristics in a rectangular cavity located in the lower wall of a two-dimensional channel whose upper wall was moved with a uniform velocity, were investigated by solving the complete Navier-Stokes equations for laminar incompressible fluid in terms of the stream function and vorticity. Numerical results were determined for a range of Reynolds numbers from 1 to 500 and for cavity aspect ratios of 0.5, 1.0 and 2.0. A circulating flow extending the whole height was observed for shallow and square cavities. For deep cavity a secondary vortex near the bottom of the cavity was also noticed.

Time-dependent solutions for the vortex flow in a square cavity bounded by three motionless walls and a fourth moving in its plane were obtained for $N_{Re}' = 10.0$ and aspect ratio of 1.0.

TABLE OF CONTENTS

page

FORWARD iii

ABSTRACT v

LIST OF ILLUSTRATIONS ix

LIST OF SYMBOLS xi

CHAPTER

I. INTRODUCTION 1

1.1 Problem Definition
1.2 Phenomenological Discussion
1.3 Historical Background

II. NUMERICAL FORMULATION 11

2.1 Governing Differential Equations
2.2 Boundary and Initial Conditions for the Governing Differential Equations
2.3 Nondimensional and Transformed Equations
2.4 Difference Formulations
2.5 Method of Solution

III. RESULTS AND DISCUSSIONS 32

IV. CONCLUSIONS 55

APPENDIX 57

REFERENCES 79

LIST OF ILLUSTRATIONS

Figure		Page
1	Problem Definition of the Flow Over a Cavity	3
2	Coordinate System and Velocity Notation	14
3	Definition of Prototype Problem	18
4	The Mapping Function	21
5	Grid Notation	25
6	Comparison with Burggraf. $N'_{Re} = 0$, Aspect Ratio = 1.0 ..	33
7	Constant Streamline Contours. $N'_{Re} = 1.0$, Aspect Ratio = 1.0	35
8	Constant Streamline Contours. $N'_{Re} = 10.0$, Aspect Ratio = 1.0	36
9	Constant Streamline Contours. $N'_{Re} = 100.0$, Aspect Ratio = 1.0	37
10	Constant Streamline Contours. $N'_{Re} = 500.0$, Aspect Ratio = 1.0	38
11	Constant Streamline Contours. $N'_{Re} = 1.0$, Aspect Ratio = 0.5	39
12	Constant Streamline Contours. $N'_{Re} = 100.0$, Aspect Ratio = 0.5	40
13	Constant Streamline Contours. $N'_{Re} = 1.0$, Aspect Ratio = 2.0	41
14	Constant Streamline Contours. $N'_{Re} = 100.0$, Aspect Ratio - 2.0	42
15	Variation of u^* with respect to z^* at $y^* = 0.9H^*$	43
16	Effect of Changing Δy^* on Vorticity at Corners	45
17	Effect of Changing Δz^* on Vorticity at Corners	46
18	Constant Streamline Contours. $N'_{Re} = 10.0$, Aspect Ratio = 1.0, $t^* = 0.02$	47
19	Constant Streamline Contours. $N'_{Re} = 10.0$, Aspect Ratio = 1.0, $t^* = 0.06$	48
20	Constant Streamline Contours. $N'_{Re} = 10.0$, Aspect Ratio = 1.0, $t^* = 0.10$	49

Figure		Page
21	Constant Streamline Contours. N'_{Re} = 10.0, Aspect Ratio = 1.0, t^* = 0.14	50
22	Constant Streamline Contours. N'_{Re} = 10.0, Aspect Ratio = 1.0, t^* = 0.31	51
23	Constant Streamline Contours. N'_{Re} = 10.0, Aspect Ratio = 1.0, t^* = 0.78	52
24	Vortex Development. N'_{Re} = 10.0, Aspect Ratio = 1.0	53

LIST OF SYMBOLS

Symbol	Description
A	Variable defined after equation (2.62)
c	$\frac{\Delta z^*}{\Delta y^*}$
c_1-c_6	Constants defined after equation (2.60)
c_r , c_z	Variables defined after equation (2.60)
C	Variable defined after equation (2.62)
D	Variable defined after equation (2.62)
$\bar{F}$	Body force vector
H	Height of the channel
H^*	Nondimensional height of the channel, $\frac{H}{L}$
H_e	Height of the cavity
H_e^*	Nondimensional height of the cavity, $\frac{H_e}{L}$
L	Length of the cavity
N_{Re}	Reynolds number, $\frac{u_m L}{\nu}$
N_{Re}'	Reynolds number, $\frac{\psi_m}{\nu}$
p	Pressure
t	Time
t^*	Nondimensional time, $\frac{\psi_m}{L^2} t$
$\bar{u}$	Velocity vector
u,v,w	Components of velocity vector, $\bar{u}$ in x, y, and z directions
u^*	Nondimensional velocity in x^* or z^* direction, $\frac{L}{\psi_m} u$
v^*	Nondimensional velocity in y^*-direction, $\frac{L}{\psi_m} v$

Symbol	Description
u_m	Velocity of the moving wall
u_m^*	Nondimensional velocity of the moving wall, $\frac{L}{\psi_m} u_m$
x	Distance along the length of the cavity
x^*	Nondimensional distance along the length of the cavity, $\frac{x}{L}$
y	Distance along the height of the cavity
y^*	Nondimensional distance along the height of the cavity, $\frac{y}{L}$
z^*	Transformed coordinate defined by equation (2.39)
$z^{*'}$	First derivative of transformation
$z^{*''}$	Second derivative of transformation
z^*_{c1}	z^*-coordinate of the upstream corner
z^*_{c2}	z^*-coordinate of the downstream corner
β_{ψ^*}	Overrelaxation parameter for ψ^*
β_{η^*}	Relaxation coefficient of η^*, defined after equation (2.60)
δ	Operator, defined on page 28
ξ, ζ, η	Components of vorticity vector, $\bar{\omega}$
η^*	Nondimensional component of vorticity in z-direction, $\frac{L^2}{\psi_m} \eta$
$\bar{\eta}^*$	First approximation of η^* at new time step
λ, μ	Coefficients of viscosity
ν	Kinematic coefficient of viscosity
ρ	Density
ψ	Stokes stream function
ψ^*	Nondimensional stream function, $\frac{\psi}{\psi_m}$

Symbol	Description
ψ_m	Maximum value of stream function
$\bar{\omega}$	Vorticity vector, $\nabla x \bar{u}$
Δy^*	Grid size in y^*-direction
Δz^*	Grid size in z^*-direction
∇	Del operator
∇^2	Laplacian operator
∇x	Curl operator
Λ	Operator, defined on page 28
Λ^2	Operator, defined on page 28

Subscripts

i	Grid point number in y^*-direction
j	Grid point number in z^*-direction
y^*	Independent variable of the operator δ or Λ or Λ^2
z^*	Independent variable of the operator δ or Λ or Λ^2

Superscripts

n	Iteration number
m	Time level

CHAPTER I
INTRODUCTION

On airfoils at large angles of attack, the adverse pressure gradient frequently causes laminar separation near the leading edge resulting in a severe stall condition. If such early separation does not occur, the flow invariably separates near the trailing edge causing much milder stall. Flow separation on aerodynamic surfaces can also be due to the presence of perturbances and cavities, as in the cases of finned surfaces, turbine flow passages, bomb bays, windows, and so on. Cavity flow problem is a special case of the general problem of separation, having most of the flow characteristics of the latter. Hence, in this study cavity flow has been investigated with the motivation of obtaining a better understanding of the phenomena of flow separation and vortex formation.

1.1 Problem Definition

The purpose of the present study is to investigate the flow characteristics in a rectangular cavity, located in the lower wall of a two-dimensional channel. The nature of the vortex formed in the cavity will depend on the Reynolds number and the height to length ratio (the aspect ratio) of the cavity. This ratio together with the channel height and length defines the geometry. The nature of the flow approaching the cavity would also influence the vortex. However, for simplification, the length of the channel was taken to be infinite and the upper wall of the channel was moved with a constant velocity thus keeping the flow approaching the cavity identical in all cases. This also facilitates defining the conditions at the upstream and the downstream boundaries of the channel.

The problem thus relates to the flow over a rectangular cavity in the lower wall of a two-dimensional infinite channel where the upper wall

is moving with a uniform velocity (Fig. 1). The flow is assumed to be laminar, incompressible and Newtonian. The results are obtained for different aspect ratios and Reynolds numbers. To magnify the phenomena of separation and vortex formation the aspect ratios were chosen to give the reattachment of the flow over the cavity and not inside it.

1.2 Phenomenological Discussion

A laminar separated flow can be defined as a separated flow in which all shear layers of importance to the problem are completely laminar. The separation and the reattachment of the flow over the cavity results in one or more eddies in the cavity (Fig. 1). One can decompose the separated flow into six more or less distinct parts: (1) separation point region, (2) free shear layer, (3) reattachment point, (4) main recirculating eddy, (5) corner eddies, and (6) external stream.

Kistler and Tan[1] define the separation point as the point where a streamline in the neighborhood of the surface breaks abruptly away from the surface. The streamline that passes through this separation point serves as a boundary between the fluid in the channel and that in the cavity. The shear layer in the neighborhood of this dividing streamline is called the free shear layer. The reattachment point is the stagnation point where part of the flow is turned back into the separated region and part moves away from this region. The flow within the separated region is made up of one or more eddies with streamlines that close on themselves.

1.3 Historical Background

During the fifteenth century Leonardo da Vinci observed and sketched recirculating eddies in the flow over various configurations. However, detailed studies of cavity flow were carried out only recently. These investigations generally consider steady plane flow of an incompressible Newtonian

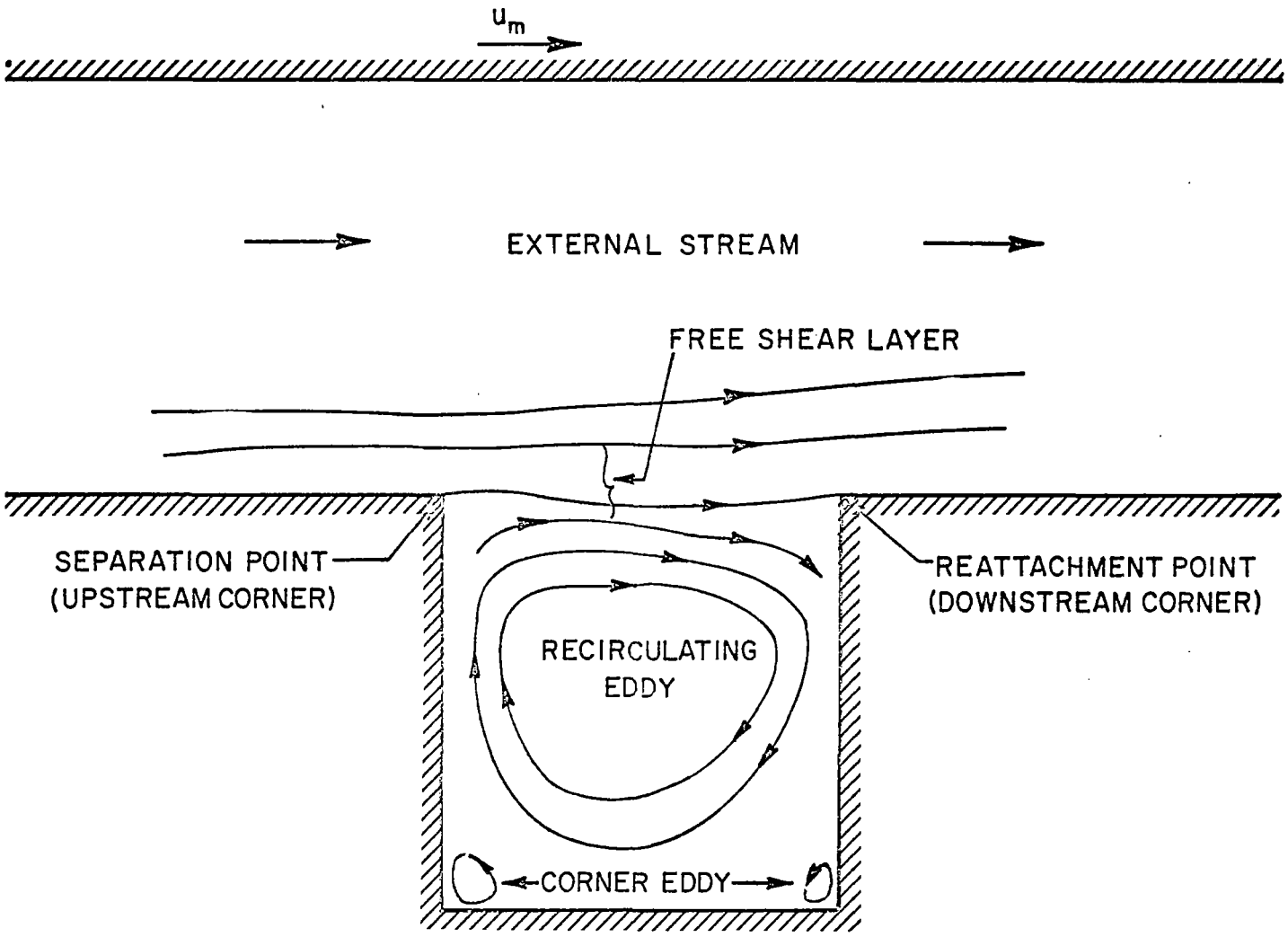

FIGURE I. PROBLEM DEFINITION OF THE FLOW OVER A CAVITY

fluid in a rectangular cavity bounded by three motionless walls and by a fourth moving in its own plane. This is the prototype of practical flow problems in which the fluid moves over a cavity.

A model proposed by Batchelor[2] has been frequently used in analyzing cavity flow. According to this model, the limiting (i.e. as μ tends to zero) laminar flow consists of a finite wake embodying a residual recirculating eddy having uniform vorticity. In cavity flow the separation region is knows to be of finite extent. For such problems, Batchelor's model appears to be correct for the limit $N_{Re} \to \infty$. This is based on the assumption that viscous effects are restricted to a thin layer along the separation streamline. Then an exact intergral theorem derived from the Navier-Stokes equations for steady flow shows that the vorticity is uniform. The specific value of the vorticity is obtained by matching the external boundary conditions using the boundary layer equations. Other theoretical models were also proposed[3] for separated flows, but with the exception of the complete Navier-Stokes equations, none has been accepted as having general sound basis.

Mills[4] carried out an analytical study of the prototype problem for a square cavity using Batchelor's model. He obtained a solution of a linearized form of Von Mises' equation for steady flow in the boundary layer for constant and varying pressures around the walls of the cavity. From this analysis the vorticity imparted to the core is obtained and is used to determine the motion in the core. Mills also performed experiments to verify his analysis. The measured velocity profiles were in qualitative agreement with the analysis. However, the measured vorticity of the inviscid core was about 1/3 the predicted value. This error was attributed to the gap between the fixed walls and the moving wall.

Burggraf[3], Mills[5] and Kawaguti[6] have solved the same problem numerically

using stream function and vorticity equation. Burggraf solved it for a square cavity for a range of Reynolds number from 0 to 400. Mills solved it for aspect ratios of 0.5, 1.0 and 2.0 for N_{Re} = 100. Whereas, Kawaguti considered aspect ratios of 0.5, 1.0 and 2.0 and a range of Reynolds number from 0 to 64.

They employed central differences to formulate the finite difference equations. Burggraf and Kawaguti chose a square mesh for all aspect ratios, whereas Mills used it for cavities having aspect ratios of 0.5 and 1.0 only. Kawaguti first calculated the vorticity at the boundary points and then the stream function and vorticity at each point in the interior. Mills utilized Liebmann's iterative technique. He went over the stream function field twice before entering the vorticity field which was also traversed twice. The boundary values of vorticity were moved by only one half of the values indicated by the boundary condition, however (as in Kawaguti's treatment) the values in the field were (mostly) given their full movement. Mills also tried a single iteration per field and found it better than the above procedure. On the other hand, Burggraf underrelaxed both stream function and vorticity in the interior of the field. During each iteration he considered points in each row progressively from right to left (the direction opposite to the motion of the moving wall), with the rows taken in order from top (moving wall) to bottom. Both Mills and Burggraf employed the corrected values as soon as they were available. Kawaguti was unable to obtain convergent solution for N_{Re} = 128.

At higher Reynolds numbers the viscous layer thickness diminishes. Burggraf observed that in this case the mesh size must be decreased for the same degree of accuracy and the relaxation (convergence) parameter must then be decreased for convergence. (Both of these imply an increased number of iterations.) He also found that for large Reynolds number the mesh size had

a strong influence on the location of the vortex center as well as on the entire flow field. In his study he allowed the maximum machine (IBM 7094) time for one case to be 30 minutes. This limitation permitted accurate solutions for $N_{Re} \leq 400$. However, approximate solutions were obtained for Reynolds numbers of up to 1000.

Mills and Kawaguti reported a circulating flow extending the whole height for shallow and square cavities. Similar results were reported by Burggraf for square cavities. Kawaguti found weak secondary flows in a large region near the bottom of a cavity of aspect ratio 2.0. However, he was unable to determine the nature of these flows because of a coarse grid and computational limitations. Mills claims to have obtained this secondary eddy at all Reynolds numbers. According to Kawaguti the center of the vortex moves downstream, as the Reynolds number increases. However, the more accurate results by Burggraf, obtained for a larger range of Reynolds number than those by Kawaguit showed that the vortex center shifted first in the downstream direction and then towards the center of the cavity as the Reynolds number was increased. Kawaguti did not observe the corner eddies. Mills reported them for aspect ratio of 1.0 and Burggraf observes them for all Reynolds numbers for the same aspect ratio.

Mills compared the theoretical results with photographs of flow patterns. There was a good correspondence between theoretical and experimental results for aspect ratio of 0.5. When the aspect ratio was 1.0, the experiments did not show the two corner eddies which he had predicted theoretically. For the aspect ratio of 2.0, a second vortex did not appear in the experiment anywhere in the range $0 \leq N_{Re} \leq 100$. (However, it appeared at $N_{Re} \sim 1000$.) These discrepancies were attributed to the difficulty of realizing in the experiment all the conditions necessary to produce a flow with such a weak vortex.

Burggraf noticed that the vorticity distribution was symmetric at $N_{Re} = 0$. At $N_{Re} = 100$, a very small inviscid core had developed around the vortex center, while at $N_{Re} = 400$, the inviscid core had grown to a diameter about 1/3 that of the cavity. The corner eddies were of triangular-shape and they had a diameter of about ten percent that of cavity at $N_{Re} = 0$. However, at $N_{Re} = 400$, the downstream eddy had grown to about 1/3 the diameter of the cavity, whereas the upstream eddy was relatively unaffected by the Reynolds number. The strength of the flow field (the maximum value of the stream function in the cavity) was practically independent of the Reynolds number.

Burggraf acquired analytical solution for the high-Reynolds-number limit ($N_{Re} \to \infty$) with the stipulation of Batchelor's uniform vorticity model. The problem was solved by the use of the finite Fourier transform. The result brings out the most serious failure of the uniform vorticity model, namely, the solution does not show the existence of secondary corner eddies.

Pan and Acrivos[7] obtained numerically the creeping flow solutions for cavities having aspect ratios from 0.25 to 5.0 using the relaxation procedure employed by Burggraf. The flow in the primary vortex (the one next to the moving wall) remained unaffected by the location of the bottom wall as long as the aspect ratio was greater than 2.0. For aspect ratio of 5.0 the first three vortices had a length to width ratio equal to 1.40. The analytical value of this ratio predicted by Moffatt[8] was 1.39.

According to Pan and Acrivos, for a square cavity, even a grid size as small as 0.01 was still too coarse to reveal the detailed streamline pattern inside the corner eddies, although it was more than adequate for the solution in the core of the cavity. The solution in the core remained practically unaffected by the changes in the structure of the corner vortices. So

an improved solution was computed after convergence in the core was assured, by subdividing the region around the corners into finer meshes and iterating further. This process of subdivision was repeated several times. It disclosed a sequence of eddies which were amazingly similar and symmetric with respect to the diagonal of the square cavity. The relative sizes and strengths of these corner vortices were in excellent agreement with analytical results obtained by Moffatt[8]. The corner vortices occupied only about 0.5 percent of the total area of the square cavity.

An experimental program was undertaken by Pan and Acrivos to study the basic features of the steady flow for different Reynolds numbers. They considered a cavity of a square section in the horizontal plane and with varying depth (height). They were not able to avoid the presence of three-dimensional fluid motions near the four intersections of the vertical sides. However, these motions did not extend into the mid-section, where to all appearances the flow was indeed two-dimensional.

Pan and Acrivos found that for a square cavity the downstream corner vortex increased in size from $N_{Re} = 0$ to $N_{Re} = 500$, in excellent agreement with Burggraf's numerical results. With a further increase in the Reynolds number, this vortex began to shrink slowly, until at $N_{Re} = 2700$ it retreated once again into the immediate neighborhood of the cavity corner. Hence, Pan and Acrivos concluded that, for a cavity of a finite ratio, to all intents and purposes the steady flow in the limit $N_{Re} \to \infty$ will consist of a single inviscid core of uniform vorticity with viscous effects being confined to infinitesimally thin boundary layers along the walls.

A cavity with aspect ratio 10.0 was used as a model for a cavity having infinite depth. As with finite cavities, the primary vortex shrunk at first as N_{Re} was increased from the creeping flow limit. Beyond $N_{Re} = 800$ the

vortex grew, with its size becoming proportional to $N_{Re}^{\frac{1}{2}}$ at Reynolds numbers between 1500 and 4000, beyond which point instabilities began to set in. It was observed that the core of the primary vortex never attained an inviscid state as $N_{Re} \to \infty$. Hence, it was concluded that for a cavity having infinite depth, the viscosity and convection play an equally important role in the momentum transfer.

O'Brien[9] has also tackled the same problem for apsect ratios of 0.5, 1.0 and 2.0, and for the range of Reynolds number from 0 to 200. She determined the numerical solution of a linearized form of the Stokes equation, a fourth order partial differential equation for the two-dimensional stream function. The result was applied to approximate the Reynolds number solution and approximations were iterated to a more accurate solution until the final answer satisfied the complete stream function equation. This procedure did not require any iteration for $N_{Re} = 1$, however, it demanded an increasing number of iterations as Reynolds number was increased. If the mesh was too large, the iterations did not converge satisfactorily and oscillated between two close sets of values. O'Brien preferred not to solve the coupled stream function and vorticity equations so as to avoid determining the boundary values of vorticity. She explains that in many cases the failure to get convergence has been traced to these boundary values.

During the course of this study the author came across the doctoral thesis of Brandt[10]. This thesis is written in Hebrew (unknown to this author) with an abstract in English. Brandt considered an infinite symmetric channel with fully-developed laminar flow at the entrance as well as exit and having recessed walls. He solved the fourth-order partial differential equation for the two-dimensional stream function. He worked with aspect ratios of 0.25, 0.5, 1.0 and 1.5. He also treated aspect ratios much less than 1.0, with a view to investigate sudden expansions and contractions in channels.

Brandt concludes that the flow in a straight channel produces a vortex flow in any rectangular recess in the channel walls; if the recess is deep enough, a main vortex is formed. His numerical procedure did not give the corner eddies for aspect ratios of 0.5, 1.0 and 1.5. The constant streamline plots for aspect ratio of 1.0 show that the dividing streamline is concave for $\overline{N}_{Re} = 0$ (based on the height of the channel and the average velocity) and convex for $\overline{N}_{Re} = 100$.

While these investigations of cavity flow contributed substantially towards a better understanding of the vortex flow, the phenomenon of flow separation coupled with the formation of vortex has not been analyzed in detail. It is well known that problems wherein the vortex motion is generated by the action of the shear stress of an outer stream, which separates and reattaches itself again, are of frequent practical occurence. The effect of the precise nature of the dividing streamline cannot safely be ignored; that is, the dividing streamline cannot be replaced by a horizontal flat plate across the top of the cavity in most of the problems. At the same time, sharp corners in the flow field may be singular points. The present work essentially deals with numerical investigation of flow separation and the formation of vortex driven by an external stream.

CHAPTER II
NUMERICAL FORMULATION

In this chapter the basic equations of hydrodynamics, suitable for the problem of cavity flow are considered along with appropriate boundary and initial conditions. Starting with the equations of mass and momentum balance for a Newtonian fluid, the assumptions necessary for obtaining useful forms of these equations are introduced. Later, to get the numerical solution of the present problem, the flow field was subdivided by a grid in the horizontal and vertical directions and at each nodal point the governing differential equations were represented by difference equations.

2.1 Governing Differential Equations

The partial differential equations of hydrodynamics for constant viscosity may be expressed as

$$\frac{\partial \rho}{\partial t} + \nabla\cdot(\rho\bar{u}) = 0 \tag{2.1}$$

(continuity or mass balance)

$$\rho\left(\frac{\partial}{\partial t} + \bar{u}\cdot\nabla\right)\bar{u} = \rho\bar{F} - \nabla p + (\lambda+\mu)\,\nabla(\nabla\cdot\bar{u}) + \mu\nabla^2\bar{u} \tag{2.2}$$

(momentum balance)

where,

t = time

ρ = density

$\bar{u}$ = velocity

$\bar{F}$ = body force per unit mass

p = pressure

μ and λ = the first and second coefficients of viscosity

The two coefficients of viscosity are related by

$$\frac{2}{3}\mu + \lambda = \kappa.$$

κ is usually referred to as the coefficient of bulk viscosity. It is customary[11] to assume that Stokes relation

$$\frac{2}{3}\mu + \lambda = 0$$

is at least approximately valid. Further, this analysis is restricted to incompressible fluids. These assumptions when applied to equations (2.1) and (2.2), yield the following equations:

$$\nabla\cdot\bar{u} = 0 \qquad \text{(continuity)} \tag{2.3}$$

$$\left(\frac{\partial}{\partial t} + \bar{u}\cdot\nabla\right)\bar{u} = \bar{F} - \frac{1}{\rho}\nabla p + \nu\nabla^2\bar{u} \qquad \text{(momentum)} \tag{2.4}$$

where

$\nu = \frac{\mu}{\rho}$ is the kinematic viscosity.

The continuity and momentum equations with appropriate boundary conditions form a complete set of equations for determining the pressure and the velocity fields. Generally, a pressure equation produced by taking the divergence of the momentum equation (2.4) is used instead of the continuity equation. The pressure equation is:

$$\frac{1}{\rho}\nabla^2 p + \nabla\cdot(\bar{u}\cdot\nabla)\bar{u} - \nabla\cdot\bar{F} = 0. \tag{2.5}$$

Another formulation of the equations of hydrodynamics may be obtained by eliminating pressure from the momentum balance equation and at the same time removing the continuity equation. This can be affected by intro-

duction of the vorticity equation and the stream function concept. Taking the curl of (2.4) and making use of (2.3) we get the vorticity equation:

$$\frac{\partial \bar{\omega}}{\partial t} - (\omega \cdot \nabla)\bar{u} + (\bar{u} \cdot \nabla)\bar{\omega} = \nabla x \bar{F} + \nu \nabla^2 \bar{\omega} \tag{2.6}$$

where the vorticity is defined by

$$\bar{\omega} = \nabla x \bar{u} \tag{2.7}$$

It is not convenient to calculate the components of the velocity vector $\bar{u}$ from (2.7). In order to circumvent this difficulty, the concept of stream function is introduced.

Aziz[12] has carried out a numerical study of cellular convection using both of the above approaches to determine the velocity field for a two-dimensional problem. He concludes that the first approach (momentum and pressure equations) yields less accurate results than the latter. The difficulty arises from the highly non-linear nature of the pressure equation and the coupling due to pressure in the momentum equations. Therefore, in this study the vorticity equation and the stream function concept are used.

The problem was formulated in Cartesian coordinates, x,y,z, with the corresponding velocity components u,v, w and vorticity components ξ,ζ,η (Fig. 2). For two-dimensional flow the vorticity components in this coordinate system are

$$\xi = \frac{\partial w}{\partial y}$$

$$\zeta = -\frac{\partial w}{\partial x} \tag{2.8}$$

$$\eta = \frac{\partial v}{\partial x} - \frac{\partial u}{\partial y}$$

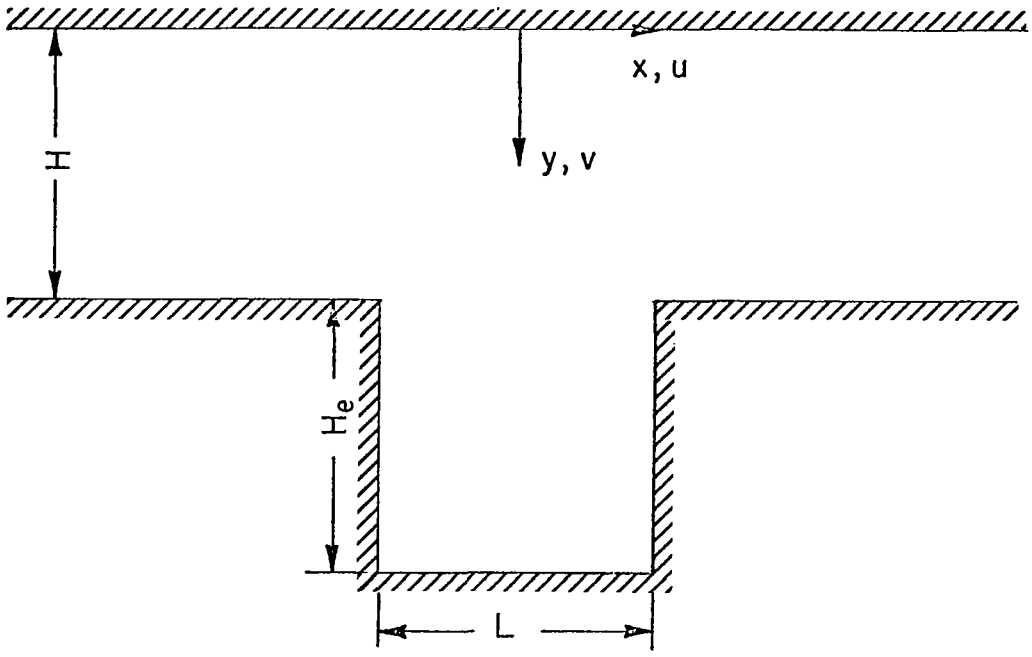

Fig. 2. Coordinate System and Velocity Notation

and the stream function, ψ , is defined by

$$u = -\frac{\partial \psi}{\partial y}$$

$$v = \frac{\partial \psi}{\partial x} \tag{2.9}$$

Introduction of these definitions of velocities in the expression for η in (2.8) gives

$$\left(\frac{\partial^2}{\partial x^2} + \frac{\partial^2}{\partial y^2}\right)\psi = \eta. \tag{2.10}$$

(stream function equation)

In addition to equation (2.10), the z-component of the vorticity equation

is used. This equation neglecting body forces is

$$\frac{\partial \eta}{\partial t} = \left(\nu \left(\frac{\partial^2}{\partial x^2} + \frac{\partial^2}{\partial y^2} \right) - \left(u \frac{\partial}{\partial x} + v \frac{\partial}{\partial y} \right) \right) \eta \qquad (2.11a)$$

(unsteady-state vorticity equation)

For steady state the above equation reduces to

$$\left(\nu \left(\frac{\partial^2}{\partial x^2} + \frac{\partial^2}{\partial y^2} \right) - \left(u \frac{\partial}{\partial x} + v \frac{\partial}{\partial y} \right) \right) \eta = 0 \qquad (2.11b)$$

(steady-state vorticity equation)

The stream function and vorticity equations with appropriate boundary and initial conditions form a complete set of equations for determining the velocity field.

2.2 Boundary and Initial Conditions for the Governing Differential Equations

The steady state problem is solved with the help of equations (2.10) and (2.11b). Since these equations are elliptic, the boundary conditions must be specified on all the boundaries. The entrance and exit of the channel are at an infinite distance from the cavity; therefore, it is assumed that at these boundaries the normal derivatives of all the functions are zero. (Alternately, the analytic values of the functions can be defined. However, past experience indicates that such analytic values may be incompatible with the numerical solution of the finite difference equations for the interior.) No slip condition is assumed on the remaining boundaries. Hence, along the moving wall the velocity of the fluid equals the velocity of the wall, whereas, on the other wall the fluid velocity is zero. Mathematically these conditions can be expressed as follows:

$$\frac{\partial \psi}{\partial x}\Big|_{x = \pm \infty} = 0 \tag{2.12}$$

$$\frac{\partial \eta}{\partial x}\Big|_{x = \pm \infty} = 0 \tag{2.13}$$

$$\psi(x, 0) = \psi_m \tag{2.14}$$

where ψ_m is the value of stream function at the moving wall.

$$\eta(x, 0) = \frac{\partial^2 \psi}{\partial y^2} \tag{2.15}$$

subject to

$$\frac{\partial \psi}{\partial y}\Big|_{y=0} = - u_m$$

where u_m is the velocity of the moving wall

$$\psi(x, H) = 0 \qquad \pm \infty \leq x \leq \pm \frac{L}{2} \tag{2.16}$$

$$\psi(x, H + H_e) = 0 \qquad - \frac{L}{2} \leq x \leq \frac{L}{2} \tag{2.17}$$

$$\psi(\pm \frac{L}{2}, y) = 0 \qquad H < y < H_e \tag{2.18}$$

$$\eta(x, H) = \frac{\partial^2 \psi}{\partial y^2} \qquad \pm \infty < x < \pm \frac{L}{2} \tag{2.19}$$

$$\eta(x, H + H_e) = \frac{\partial^2 \psi}{\partial y^2} \qquad - \frac{L}{2} < x < \frac{L}{2} \tag{2.20}$$

$$\eta(\pm \frac{L}{2}, y) = \frac{\partial^2 \psi}{\partial x^2} \qquad H < y < H_e \tag{2.21}$$

$$\eta(\pm \frac{L}{2}, H) = \frac{\partial^2 \psi}{\partial x^2} + \frac{\partial^2 \psi}{\partial y^2} \tag{2.22}$$

In equations (2.19) to (2.22) the second derivatives are evaluated subject to the condition that the first derivatives, that is, the velocities are zero. (This corresponds to the no slip assumption.)

The numerical procedure was varified by reproducing Burggraf's results for the prototype problem (Fig. 3), with the boundary conditions (2.23) to (2.25) given below and again with the no slip assumption.

$$\psi(\pm \frac{L}{2}, y) = 0 \tag{2.23}$$

$$\psi(x, 0) = 0 \tag{2.24}$$

$$\psi(x, H_e) = 0 \tag{2.25}$$

$$\eta(x, 0) = \frac{\partial^2 \psi}{\partial y^2} \tag{2.26}$$

$$\eta(x, H_e) = \frac{\partial^2 \psi}{\partial y^2} \tag{2.27}$$

$$\eta(\pm \frac{L}{2}, y) = \frac{\partial^2 \psi}{\partial x^2} \tag{2.28}$$

The formation of the vortex was studied by solving the stream function equation (2.10) and the unsteady-state vorticity equation (2.11a) for the prototype problem. The boundary conditions are the same as equations (2.23) to (2.28) for all time t. In addition to these, initial conditions are specified in the interior of the entire field because equation (2.11a) is parabolic with respect to time.

$$\psi(x, y, 0) = 0 \tag{2.29}$$

$$\eta(x, y, 0) = 0 \tag{2.30}$$

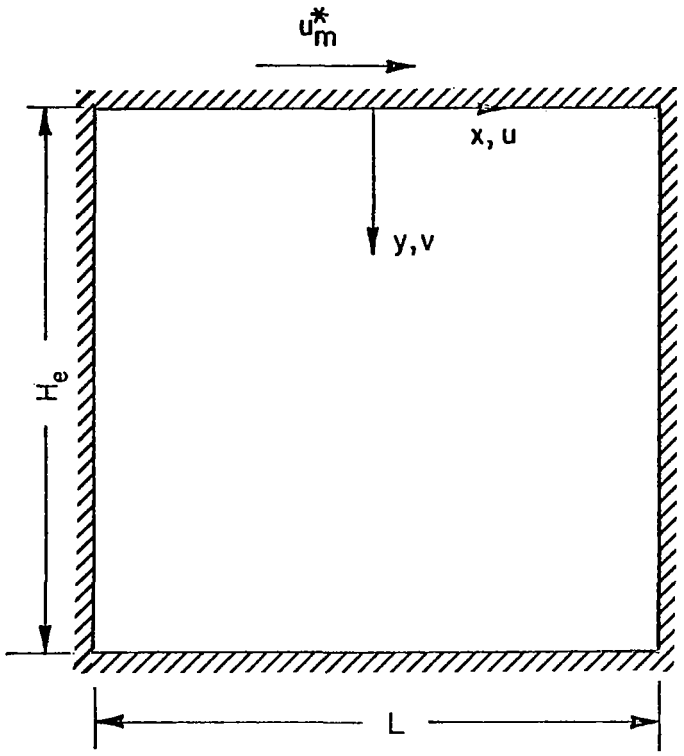

Fig. 3. Definition of the Prototype Problem

2.3 Nondimensional and Transformed Equations

The equations are made dimensionless using the length of the cavity, L, and the stream function at the moving wall, ψ_m, as reference dimensions.

$$x^* = \frac{x}{L} \qquad u^* = \frac{L}{\psi_m} u$$

$$y^* = \frac{y}{L} \qquad v^* = \frac{L}{\psi_m} v \qquad (2.31)$$

$$\psi^* = \frac{\psi}{\psi_m} \qquad \eta^* = \frac{L^2}{\psi_m} \eta$$

$$t^* = \frac{\psi_m}{L^2} t$$

where the nondimensional quantities are designated by asterisks.

The nondimensional equations are

$$\left(\frac{\partial^2}{\partial x^{*2}} + \frac{\partial^2}{\partial y^{*2}}\right)\psi^* = \eta^* \tag{2.32}$$

$$N'_{Re}\ \frac{\partial \eta^*}{\partial t^*} = \left(\frac{\partial^2}{\partial x^{*2}} + \frac{\partial^2}{\partial y^{*2}} - N'_{Re}\left(u^*\frac{\partial}{\partial x^*} + v^*\frac{\partial}{\partial y^*}\right)\right)\eta^* \tag{2.33a}$$

$$\left(\frac{\partial^2}{\partial x^{*2}} + \frac{\partial^2}{\partial y^{*2}} - N'_{Re}\left(u^*\frac{\partial}{\partial x^*} + v^*\frac{\partial}{\partial y^*}\right)\right)\eta^* = 0 \tag{2.33b}$$

where

$$N'_{Re} = \frac{\psi_m}{\nu} \tag{2.34}$$

By definition

$$u = -\frac{\partial \psi}{\partial y}$$

and

$$\psi_m = -\int_o^H u\,dy$$

Also, for a Couette flow

$$u = u_m\left(1 - \frac{y}{H}\right).$$

Hence,

$$\psi_m = \frac{u_m H}{2} \tag{2.35}$$

if

$$\psi(x, H) = 0$$

Note

$$\psi_m \equiv \frac{u_m L}{2} \quad \text{for the prototype problem}$$

Therefore,

$$N'_{Re} = \frac{u_m H}{2\nu} \tag{2.36}$$

The nondimensional equations may be transformed from the physical plane (x^*, y^*) to any new plane $(z^*(x^*), y^*)$ as follows.

$$\left(\left(\frac{dz^*}{dx^*}\right)^2 \frac{\partial^2}{\partial z^{*2}} + \frac{d^2 z^*}{dx^{*2}} \frac{\partial}{\partial z^*} + \frac{\partial^2}{\partial y^{*2}}\right) \psi^* = \eta^* \tag{2.37}$$

$$N'_{Re} \frac{\partial \eta^*}{\partial t^*} = \left(\left(\frac{dz^*}{dx^*}\right)^2 \frac{\partial^2}{\partial z^{*2}} + \frac{d^2 z^*}{dx^{*2}} \frac{\partial}{\partial z^*} + \frac{\partial^2}{\partial y^{*2}} - N'_{Re}\left(u^* \frac{dz^*}{dx^*} \frac{\partial}{\partial z^*} + v^* \frac{\partial}{\partial y^*}\right)\right) \eta^* \tag{2.38a}$$

and

$$\left(\left(\frac{dz^*}{dx^*}\right)^2 \frac{\partial^2}{\partial z^{*2}} + \frac{d^2 z^*}{dx^{*2}} \frac{\partial}{\partial z^*} + \frac{\partial^2}{\partial y^{*2}} - N'_{Re}\left(u^* \frac{dz^*}{dx^*} \frac{\partial}{\partial z^*} + v^* \frac{\partial}{\partial y^*}\right)\right) \eta^* = 0 \tag{2.38b}$$

The equations were transformed so that the infinite channel in the physical plane can be contracted to a finite length in the transformed plane. At the same time the transformation was so chosen that the neighborhood of each of the convex corners was expanded. Thus a uniform grid in the transformed plane is equivalent to a finer grid near the convex corners in the physical plane. This facilitates the study of the rapid changes in the flow

field near these corners. The transformation chosen is defined by

$$z^* = \frac{1 + \tanh\, a(x^* + 0.5)}{1 + \tanh\,(0.5a)} \tag{2.39}$$

where 'a' is a constant. This transformation maps $-\infty < x^* < 0{\cdot}0$ into $0{\cdot}0 < z^* < 1.0$, with a point of inflection at $x^* = -0.5$ which is the upstream corner.

The function can be extended for the domain $0 < x^* < \infty$ by assuming that it is antisymmetric about $z^* = 1.0$, that is

$$1 - f(x^*) = f(-x^*) - 1 \tag{2.40}$$

The mapping function thus defined (Fig. 4) and its first derivative are continuous. However, the second derivative has a finite jump discontinuity with an average value of zero at $x^* = 0$.

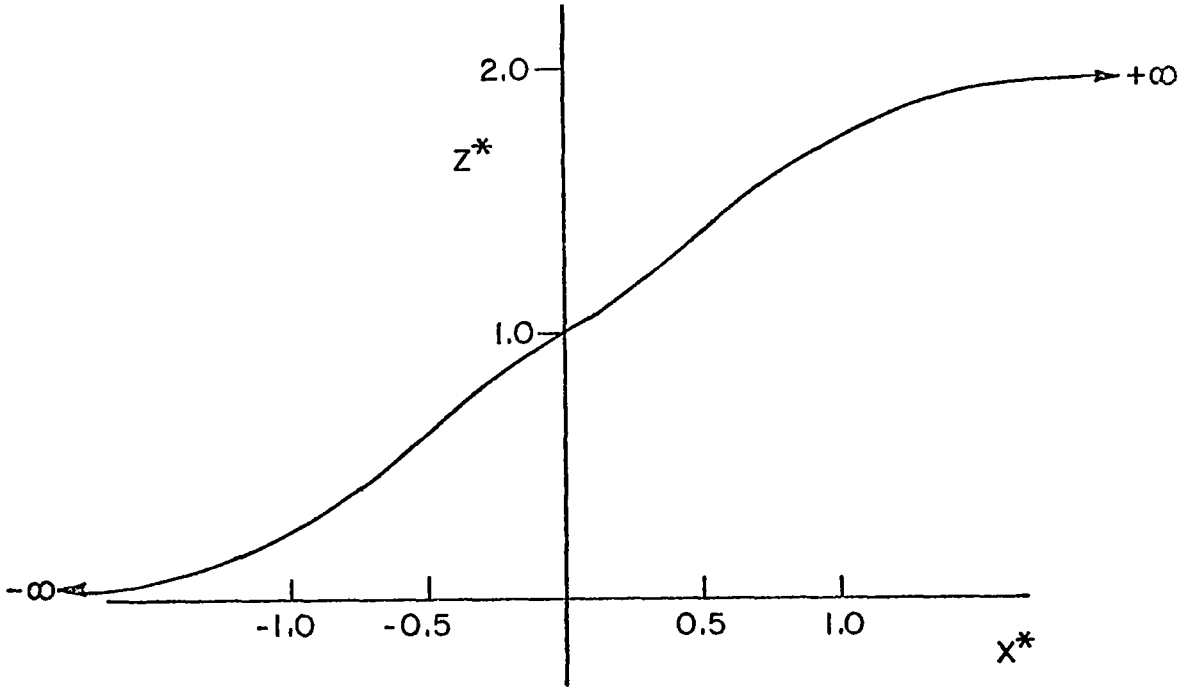

Fig. 4. The Mapping Function

Finally, the boundary conditions listed in the previous section are rewritten in the nondimensional and transformed forms. Equations (2.12) to (2.22) for the channel flow are considered first.

$$\frac{\partial \psi^*}{\partial z^*} = 0 \qquad (2.41)$$

and

$$\frac{\partial \eta^*}{\partial z^*} = 0 \qquad (2.42)$$

at inlet and exit

Note, $\frac{dz^*}{dx^*} = 0 \qquad x = \pm \infty$

$$\psi^*(z^*, 0) = 1.0 \qquad (2.43)$$

$$\eta^*(z^*, 0) = \frac{\partial^2 \psi^*}{\partial y^{*2}} \qquad (2.44)$$

subject to

$$\left.\frac{\partial \psi^*}{\partial y^*}\right|_{y=0} = -\frac{u_m L}{\psi_m}$$

$$\psi(z^*, H^*) = 0 \qquad 0 \le z^* \le z^*_{c1} \qquad (2.45)$$

$$z^*_{c2} \le z^* \le 2.0$$

where z^*_{c1} and z^*_{c2} are the values of the transformed coordinates of the upstream and downstream corners, respectively.

$$\psi^*(z^*, H^* + H_e^*) = 0 \qquad z_{c1}^* \le z^* \le z_{c2}^* \tag{2.46}$$

$$\psi^*(z_{c1}^*, y^*) = 0 \qquad H^* < y^* < H_e^* \tag{2.47a}$$

$$\psi^*(z_{c2}^*, y^*) = 0 \qquad H^* < y^* < H_e^* \tag{2.47b}$$

$$\eta^*(z^*, H^*) = \frac{\partial^2 \psi^*}{\partial y^{*2}} \qquad 0 < z^* < z_{c1}^*$$

$$z_{c2}^* < z^* < 2.0 \tag{2.48}$$

$$\eta^*(z^*, H^* + H_e^*) = \frac{\partial^2 \psi^*}{\partial y^{*2}} \qquad z_{c1}^* < z^* < z_{c2}^* \tag{2.49}$$

$$\eta^*(z_{c1}^*, y^*) = \left(\frac{dz^*}{dx^*}\right)^2 \frac{\partial^2 \psi^*}{\partial z^{*2}} \qquad H^* < y^* < H_e^* \tag{2.50a}$$

Note ,

$$\frac{d^2 z^*}{dx^{*2}} = 0 \qquad x^* = \pm 0.5$$

$$\eta^*(z_{c2}^*, y^*) = \left(\frac{dz^*}{dx^*}\right)^2 \frac{\partial^2 \psi^*}{\partial z^{*2}} \qquad H^* < y^* < H_e^* \tag{2.50b}$$

$$\eta^*(z_{c1}^*, H^*) = \left(\frac{dz^*}{dx^*}\right)^2 \frac{\partial^2 \psi^*}{\partial z^{*2}} + \frac{\partial^2 \psi^*}{\partial y^{*2}} \tag{2.51}$$

$$\eta^*(z_{c2}^*, H^*) = \left(\frac{dz^*}{dx^*}\right)^2 \frac{\partial^2 \psi^*}{\partial z^{*2}} + \frac{\partial^2 \psi^*}{\partial y^{*2}} \tag{2.52}$$

In a similar manner the boundary conditions for the prototype problem are nondimensionalized and transformed. The same mapping function (equation (2.39)) was employed. Equations (2.23) to (2.28) became

$$\psi^*(z^*_{c1}, y^*) = 0 \tag{2.53a}$$

$$\psi^*(z^*_{c2}, y^*) = 0 \tag{2.53b}$$

$$\psi^*(z^*, 0) = 0 \tag{2.54}$$

$$\psi^*(z^*, H_e^*) = 0 \tag{2.55}$$

$$\eta^*(z^*, 0) = \frac{\partial^2 \psi^*}{\partial y^{*2}} \tag{2.56}$$

$$\eta^*(z^*, H_e^*) = \frac{\partial^2 \psi^*}{\partial y^{*2}} \tag{2.57}$$

$$\eta^*(z^*_{c1}, y^*) = \left(\frac{dz^*}{dx^*}\right)^2 \frac{\partial^2 \psi^*}{\partial z^{*2}} \tag{2.58a}$$

$$\eta^*(z^*_{c2}, y^*) = \left(\frac{dz^*}{dx^*}\right)^2 \frac{\partial^2 \psi^*}{\partial z^{*2}} \tag{2.58b}$$

2.5 Method of Solution

Aziz[12] has reviewed the numerical methods applied to viscous hydrodynamics problems similar to the one considered here. According to him alternating direction implicit methods (A.D.I.) are very effective in solving non-linear parabolic partial differential equations. He also solved a three-dimensional natural convection problem with the A.D.I. method. Hence, in this work the unsteady state vorticity equation is treated similarly.

As mentioned earlier, Mills solved the elliptic equations with Liebmann's method. Burggraf and Kawaguti used a slight modification of Liebmann's technique. In this work the steady state solution follows the treatment of Lavan and Fejer[13], which is also a modification of Liebmann's method.

The flow field is divided in rectangular grid in the transformed plane, Fig. 5, and the finite difference equations are solved for the values of the dependent variables at the nodal points.

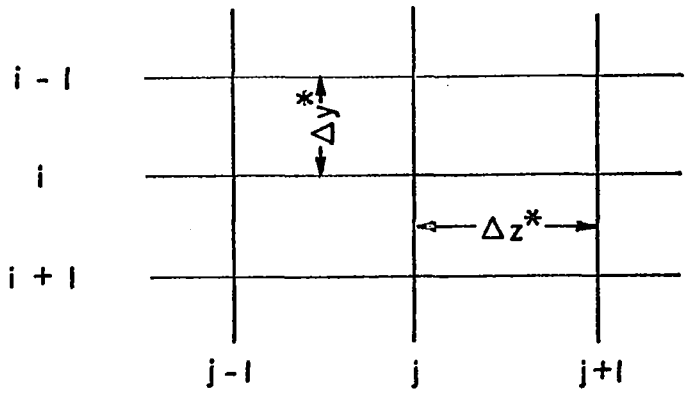

Fig. 5. Grid Notation

Consider first the numerical solution of the steady-state vorticity and stream function equations. In the stream function equation the derivatives are substituted by central differences. In the vorticity equation the second order derivatives are replaced by central differences; the first order derivatives are approximated by backward or forward differences depending on whether the coefficients of these derivatives are positive or negative, as explained by Lavan and Fejer. The finite difference form of equations (2.37) and (2.38b) are:

$$\psi^{*n+1}_{i,j} = \psi^{*n}_{i,j} + \beta_{\psi^*} \left\{ \frac{1}{2.0\,(z^{*\prime})^2 + c^2} \left(\psi^{*n}_{i,j+1} \left((z^{*\prime})^2 + \frac{z^{*\prime\prime}\,\Delta z^*}{2.0} \right) + \psi^{*n+1}_{i,j-1} \left((z^{*\prime})^2 - \frac{z^{*\prime\prime}\,\Delta z^*}{2.0} \right) + \psi^{*n}_{i+i,j} \left(\frac{\Delta z^*}{\Delta y^*} \right)^2 + \psi^{*n+1}_{i-1,j} \left(\frac{\Delta z^*}{\Delta y^*} \right)^2 - \Delta z^{*2}\, \eta^*_{i,j} \right) - \psi^{*n}_{i,j} \right\} \qquad (2.59)$$

$$
\begin{aligned}
\eta^{*n+1}_{i,j} = \eta^{*n}_{i,j} + \beta_{\eta^*} \Bigg\{ & (1.0 + c_1\, c_r)\, \eta^{*n+1}_{i+1,j} + (1.0 + c_2\, c_r)\, \eta^{*n}_{i-1,j} \\
& + \left(\left(\frac{\Delta y^*}{\Delta z^*} z^{*\prime} \right)^2 + c_4\, c_z \right) \eta^{*n}_{i,j+1} \\
& + \left(\left(\frac{\Delta y^*}{\Delta z^*} z^{*\prime} \right)^2 + c_5\, c_z \right) \eta^{*n+1}_{i,j-1} \\
& - \left(2.0 + 2.0 \left(\frac{\Delta y^*}{\Delta z^*} z^{*\prime} \right)^2 + c_3\, c_r + c_6\, c_z \right) \eta^{*n}_{i,j} \Bigg\}
\end{aligned}
\tag{2.60}
$$

where

n = the level of iteration

β_{ψ^*} = overrelaxation parameter

$c = \dfrac{\Delta z^*}{\Delta y^*}$

$z^{*\prime}$ = the first derivative of transformation

$z^{*\prime\prime}$ = the second derivative of transformation

$c_r = N'_{Re} v^* \Delta y^*$

$c_z = (- z^{*\prime\prime} + N'_{Re} z^{*\prime} u^*) \dfrac{\Delta y^{*2}}{\Delta z^*}$

$\beta_{\eta^*} = 1.0/(2.0 + 2.0 (\dfrac{\Delta y^*}{\Delta z^*} z^{*\prime})^2 + (c_1 + 2.0\, c_2)\, c_r + (2.0\, c_4 + c_5)\, c_z)$

$c_1 = -1$ and $c_2 = 0$ if $c_r < 0$

$c_1 = 0$ and $c_2 = 1$ if $c_r > 0$

$c_4 = -1$ and $c_5 = 0$ if $c_z < 0$

$c_4 = 0$ and $c_5 = 1$ if $c_z > 0$

$c_3 = c_1 + c_2$

$c_6 = c_4 + c_5$

These finite difference equations ((2.59) and (2.60)) were solved along with the appropriate boundary conditions. Initial values were assigned to

all nodal points and improved values of these functions were obtained by successively scanning over the grid points once with each of the equations. The scanning proceeded in the direction of increasing z^* and decreasing y^*. This procedure was repeated until the maximum error (residue) in the field was smaller than some prescribed value.

Now, consider the A.D.I. method for equation (2.38a). The procedure used is a perturbation of the Crank-Nicholson scheme which is defined as

$$\frac{\partial^2 f}{\partial q^2} = \frac{1}{2}\left(\Lambda^2_q f^m + \Lambda^2_q f^{m+1}\right) \tag{2.61}$$

where the second derivative is defined at time level m and where

$$\Lambda^2_q f = \frac{f_{k+1} + f_{k-1} - 2 f_k}{\Delta q^2}$$

This scheme requires an implicit method for the solution of finite difference equations. The perturbed technique employed here was formulated by Douglas[11] for linear and mildly nonlinear parabolic equations. He has shown that for a cubic region his method is stable for any positive time step. However, an exact stability analysis for nonlinear equation is lacking.

Before going into details of the numerical method, equation (2.38a) is rewritten in a different form and some useful quantities are defined.

$$N'_{Re}\frac{\partial \eta^*}{\partial t^*} = A\frac{\partial^2 \eta^*}{\partial z^{*2}} + \frac{\partial^2 \eta^*}{\partial y^{*2}} + C\frac{\partial \eta^*}{\partial z^*} + D\frac{\partial \eta^*}{\partial y^*} \tag{2.62}$$

where

$$A = (z^{*\prime})^2$$

$$C = -\left(N'_{Re} u^* z^{*\prime} - z^{*\prime\prime}\right)$$

$$D = -N'_{Re} v^*$$

Let

$$\Lambda_{z^*}\eta^{*m} = \frac{\eta^{*m}_{i,j+1} - \eta^{*m}_{i,j-1}}{2\Delta z^*}$$

$$\Lambda_{y^*}\eta^{*m} = \frac{\eta^{*m}_{i+1,j} - \eta^{*m}_{i-1,j}}{2\Delta y^*}$$

$$\Lambda^2_{z^*}\eta^{*m} = \frac{\eta^{*m}_{i,j+1} + \eta^{*m}_{i,j-1} - 2\eta^{*m}_{i,j}}{\Delta z^{2*}}$$

$$\Lambda^2_{y^*}\eta^{*m} = \frac{\eta^{*m}_{i+1,j} + \eta^{*m}_{i-1,j} - 2\eta^{*m}_{i,j}}{\Delta y^{*2}}$$

$$\delta_{z^*}\eta^{*m} = (A\Lambda^2_{z^*} + C\Lambda_{z^*})\ \eta^{*m}$$

$$\delta_{y^*}\eta^{*m} = (\Lambda^2_{y^*} + D\Lambda_{y^*})\ \eta^{*m}$$

The numerical solution of equation (2.62) can be obtained at t^{*m+1} from the known solution at t^*_m by

$$\frac{1}{2}\delta_{z^*}(\bar{\eta}^{*m+1} + \eta^{*m}) + \delta_{y^*}\eta^{*m} = N'_{Re}\ \frac{\bar{\eta}^{*m+1} - \eta^{*m}}{\Delta t^*} \qquad (2.63)$$

where $\bar{\eta}^{*m+1}$ is the first estimate of vorticity at t^{*m+1}. The final value is calculated from

$$\frac{1}{2}\delta_{z^*}(\bar{\eta}^{*m+1} + \eta^{*m}) + \frac{1}{2}\delta_{y^*}(\eta^{*m+1} + \eta^{*m}) = N'_{Re}\ \frac{\eta^{*m+1} - \eta^{*m}}{\Delta t^*} \qquad (2.64)$$

Rearranging equation (2.63),

$$\left\{\delta_{z}^{*} - \frac{2.0\ N'_{Re}}{\Delta t^{*}}\right\}\bar{\eta}^{*m+1} = -\left\{\delta_{z}^{*} + 2.0\ \delta_{y}^{*} + \frac{2.0\ N'_{Re}}{\Delta t^{*}}\right\}\eta^{*m} \qquad (2.65)$$

Substracting equation (2.63) from equation (2.64) and rearranging

$$\left\{\delta_{y}^{*} - \frac{2.0\ N'_{Re}}{\Delta t^{*}}\right\}\eta^{*m+1} = \delta_{y}^{*}\,\eta^{*m} - \frac{2.0\ N'_{Re}}{\Delta t^{*}}\,\bar{\eta}^{*m+1} \qquad (2.66)$$

Equations (2.65) and (2.66) reduce to

$$\left(\frac{A}{\Delta z^{*2}} + \frac{C}{2.0\ \Delta z^{*}}\right)\bar{\eta}^{*m+1}_{i,j+1} + \left(-\frac{2.0A}{\Delta z^{*2}} - \frac{2.0\ N'_{Re}}{\Delta t^{*}}\right)\bar{\eta}^{*m+1}_{i,j}$$

$$+\left(\frac{A}{\Delta z^{*2}} - \frac{C}{2.0\Delta z^{*}}\right)\bar{\eta}^{*m+1}_{i,j-1}$$

$$=\left(-\frac{A}{\Delta z^{*}} - \frac{C}{2.0\Delta z^{*}}\right)\eta^{*m}_{i,j+1}$$

$$+\left(-\frac{A}{\Delta z^{*2}} + \frac{C}{2.0\Delta z^{*}}\right)\eta^{*m}_{i,j-1}$$

$$+\left(-\frac{2.0}{\Delta y^{*2}} - \frac{D}{\Delta y^{*}}\right)\eta^{*m}_{i+1,j}$$

$$+\left(-\frac{2.0}{\Delta y^{*2}} + \frac{D}{\Delta y^{*}}\right)\eta^{*m}_{i-1,j}$$

$$+\left(\frac{2.0\ A}{\Delta z^{*2}} + \frac{4.0}{\Delta y^{*2}} - \frac{2.0\ N'_{Re}}{\Delta t^{*}}\right)\eta^{*m}_{i,j} \qquad (2.67)$$

$$\left(\frac{1}{\Delta y^{*2}} + \frac{D}{2.0\Delta y^{*}}\right) \eta^{*m+1}_{i+1,j} + \left(-\frac{2.0}{\Delta y^{*2}} - \frac{2.0\ N'_{Re}}{\Delta t^{*}}\right) \eta^{*m+1}_{i,j}$$

$$+ \left(\frac{1}{\Delta y^{*2}} - \frac{D}{2.0\Delta y^{*}}\right) \eta^{*m+1}_{i-1,j}$$

$$= \left(\frac{1}{\Delta y^{*2}} + \frac{D}{2.0\Delta y^{*}}\right) \eta^{*m}_{i+1,j}$$

$$+ \left(\frac{1}{\Delta y^{*2}} - \frac{D}{2.0\Delta y^{*}}\right) \eta^{*m}_{i-1,j}$$

$$+ \left(-\frac{2.0}{\Delta y^{*2}}\right) \eta^{*m}_{i,j} - \frac{2.0\ N'_{Re}}{\Delta t^{*}}\ \bar{\eta}^{*m+1}_{i,j} \qquad (2.68)$$

Each of the above two equations involves the solution of a tridiagonal system of linear algebraic equations.

The time dependent vorticity equations ((2.67) and (2.68)) and the stream function equation (2.59) along with the appropriate boundary conditions were solved to determine the transient solution for the prototype problem. At all nodal points initial values were assigned. These values were either for $t^{*} = 0$ or for t^{*m}. In the former case they would be zero and in the latter case they would be the previously calculated values. The vorticity was first calculated on the boundaries and then in the interior by the A.D.I. method. The stream function equation was completely relaxed using the values of vorticity at the new time. This procedure was repeated for a desired number of time levels.

The vorticity at the boundaries and the coefficient of the first order terms in the vorticity equation always lagged one time step behind the rest

of the field. However, all the values in the field might be iterated at the same time step until the boundary values of vorticity did not change more than a prescribed limit. This would make the computer time and cost prohibitive; as a result, this refinement in the solution was not considered.

As mentioned before, vorticity at the solid boundaries was calculated from the second derivative of stream function. The stream function was expanded about the boundary under consideration in a Taylor series, and the appropriate value of the velocity was substituted for the first derivatives. The resulting expression was solved for the second derivative to get its finite difference form. However, for the channel flow at the entrance and the exit the normal derivatives of vorticity as well as stream function were assumed to be zero. These conditions are enforced by treating the boundary points as interior points and reflecting the values of the function at the interior points (the ones next to the boundary) to the points outside the boundary.

CHAPTER III
RESULTS AND DISCUSSION

It is generally desirable to check the validity of a numerical procedure by comparison with some known results. Therefore, first the prototype problem was solved for creeping flow in a square cavity. The results are presented as contours of constant stream function (i.e. as streamlines) along with Burggraf's solution for the same case (Fig. 6). (In the present work the contours of constant streamlines were obtained by graphical interpolation whereas Burggraf employed numerical interpolation.) Good agreement is indicated in Fig. 6 in the entire flow field with the exception of the region near the center of the vortex, where the maximum values of the stream function in the two cases differ by 4.3 per cent. This variation is probably due to the coarser grid (11 x 13 points) and the use of one-sided differences for first derivatives as compared with Burggraf's finer grid (50 x 50) and central differences. (The one-sided differences were chosen because the stability analysis by Lavan and Fejer shows the central differences to be unstable for numerical solutions of channel flow.)

After partially confirming the validity of the numerical procedure, it was utilized in the main investigation of the flow in a cavity along the wall of a channel. The grid size was 0.1 and 0.0625 in y^* and z^*-direction, respectively. The stream function and vorticity values were relaxed until the residues were smaller than 1.5×10^{-6} and 2.5×10^{-4}, respectively. The height of the channel and the length of the cavity were always kept the same but the height of the cavity was varied to obtain the aspect ratios of 0.5 1.0 and 2.0.

It should be noted that in the prototype problem the boundary layer thickness along the walls of the cavity becomes thinner as Reynolds number is

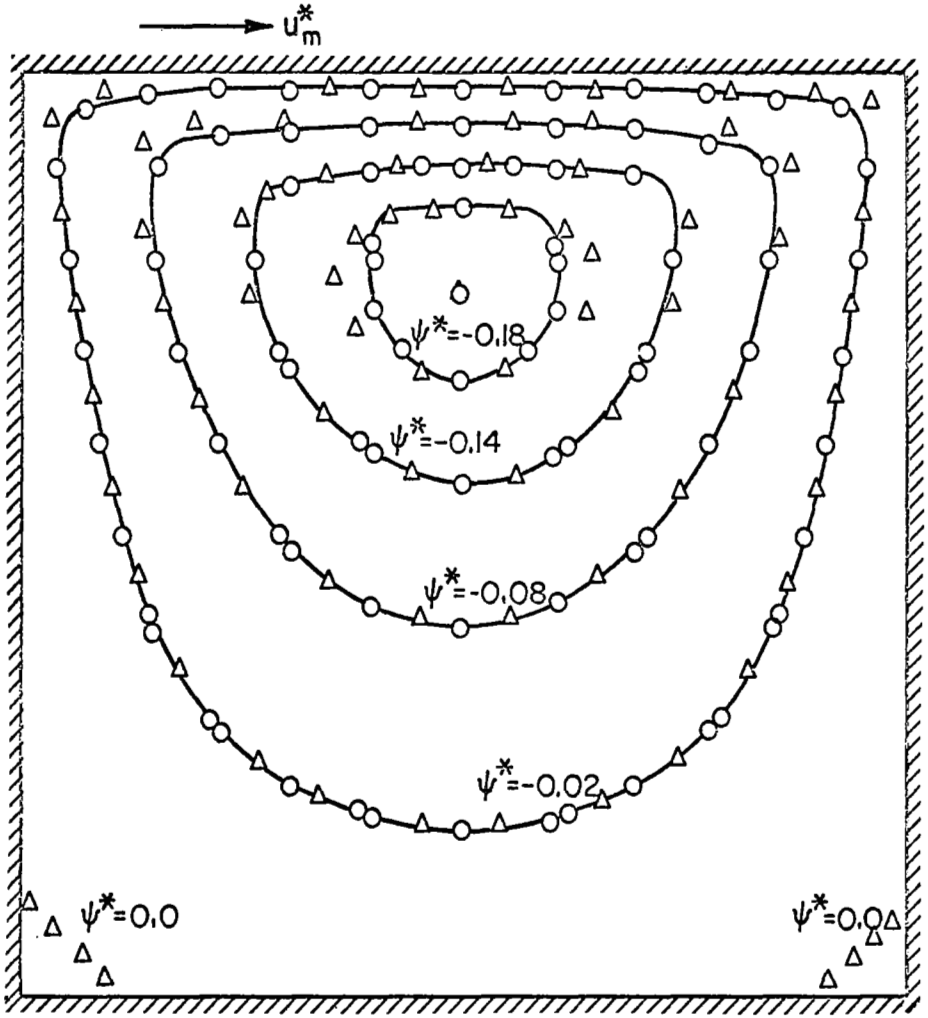

Δ BURGGRAF (REF. 3)

ψ_m^* =-0.1911 FOR PRESENT WORK

ψ_m^* =-0.2 FOR BURGGRAF'S WORK

FIGURE 6. COMPARISON WITH BURGGRAF. $N_{Re}' = 0$, ASPECT RATIO= 1.0.

increased and the proper representation of the flow field would require finer and finer mesh sizes. In this problem Reynolds number is directly proportional to the velocity of the moving wall, while in the present problem it is proportional to the velocity of upper channel wall. Hence a large Reynolds number (say 1000) in the present problem corresponds to a much smaller Reynolds number based on the average velocity in the free shear layer on top of the cavity. It is therefore believed that the results obtained using 99 grid points inside the cavity are accurate for the entire range of Reynolds numbers investigated (1 - 500).

Constant streamline plots are shown in Figs. 7 to 10 and in Figs. 11 and 12 for the aspect ratios of 1.0 and 0.5, respectively. Only one vortex is observed in these cases. An increase in the Reynolds number affects the vortex flow as follows: (1) the strength of the vortex first increases and then decreases; (2) the vortex center shifts downstream and in an upward direction; (3) the streamlines in the free shear layer cluster together; and (4) the streamline dividing the cavity flow and the channel flow is concave at low Reynolds numbers and convex at high Reynolds numbers.

Two vortices, one stronger than the other, are observed (Figs. 13 and 14) for a deep cavity having an aspect ratio of 2.0. The primary vortex extends to a depth of 75.0 per cent and 70.9 per cent of the cavity height for $N'_{Re} = 1.0$ and $N'_{Re} = 100.0$, respectively. This vortex has a height to legnth ratio of 1.464, for $N'_{Re} = 1.0$ and 1.460 for $N'_{Re} = 100.0$. The numerical creeping flow solution of Pan and Acrivos, for the prototype problem with the same aspect ratio predicts this ratio to be 1.4.

The effect of the presence of the cavity on the external stream (the channel flow) is shown in Fig. 15. The variation of velocity u^* with respect to z^*, at one grid point away from the wall having the cavity is given. At

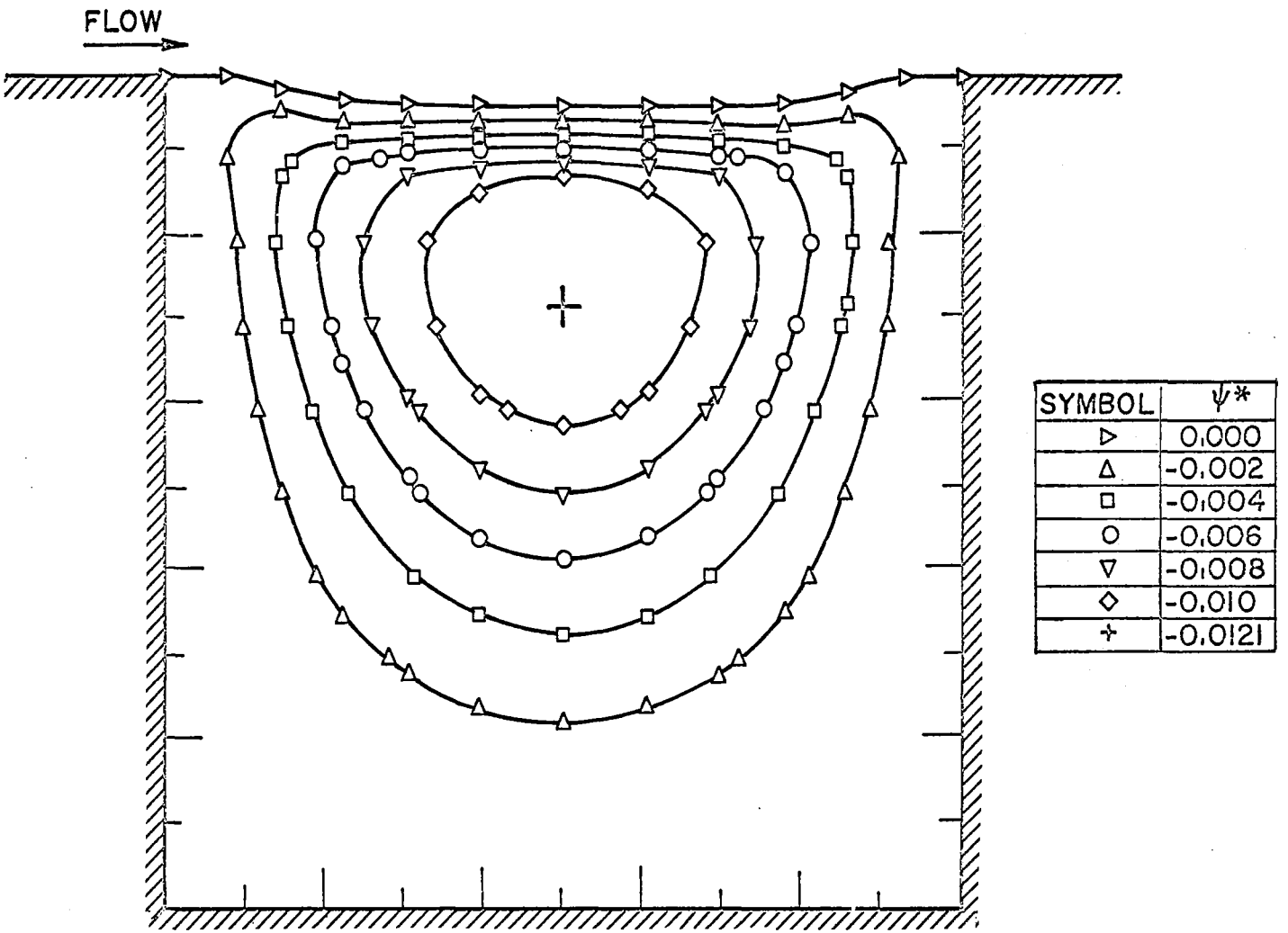

FIGURE 7. CONSTANT STREAMLINE CONTOURS. N_{Re}' = 1.0, ASPECT RATIO = 1.0.

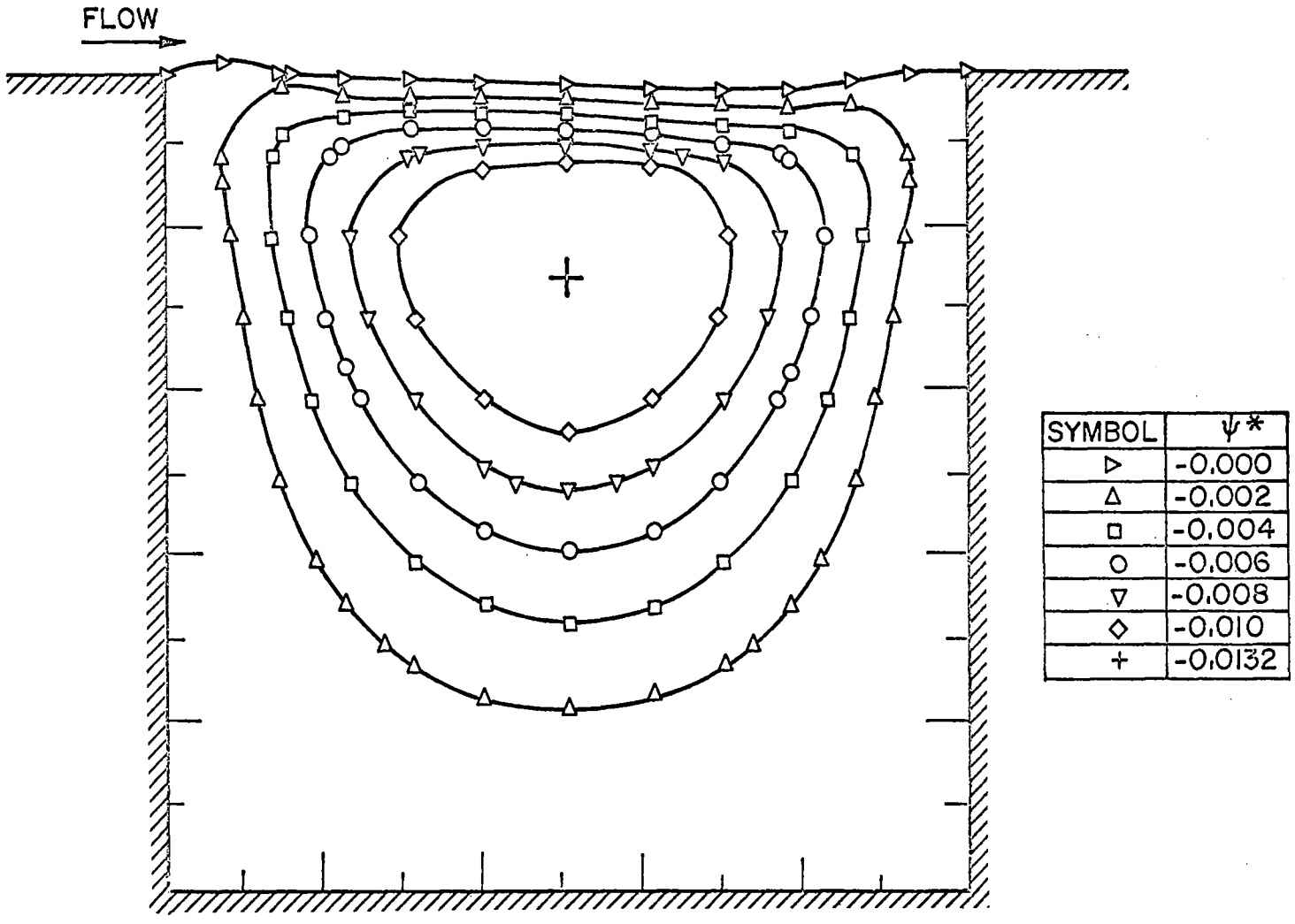

FIGURE 8. CONSTANT STREAMLINE CONTOURS. N_{Re}' = 10.0, ASPECT RATIO = 1.0.

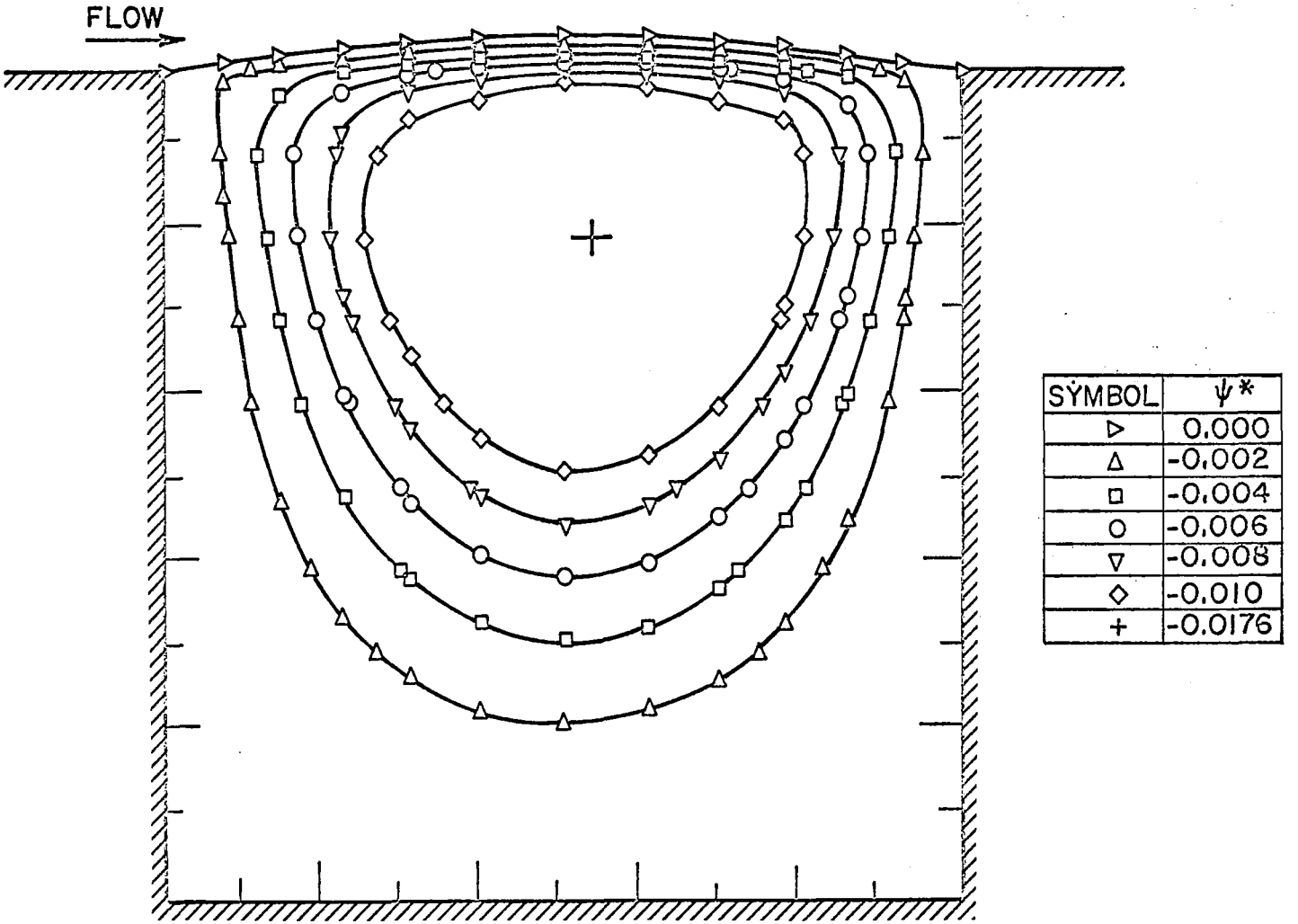

FIGURE 9. CONSTANT STREAMLINE CONTOURS. $N_{Re}' = 100.0$, ASPECT RATIO = 1.0.

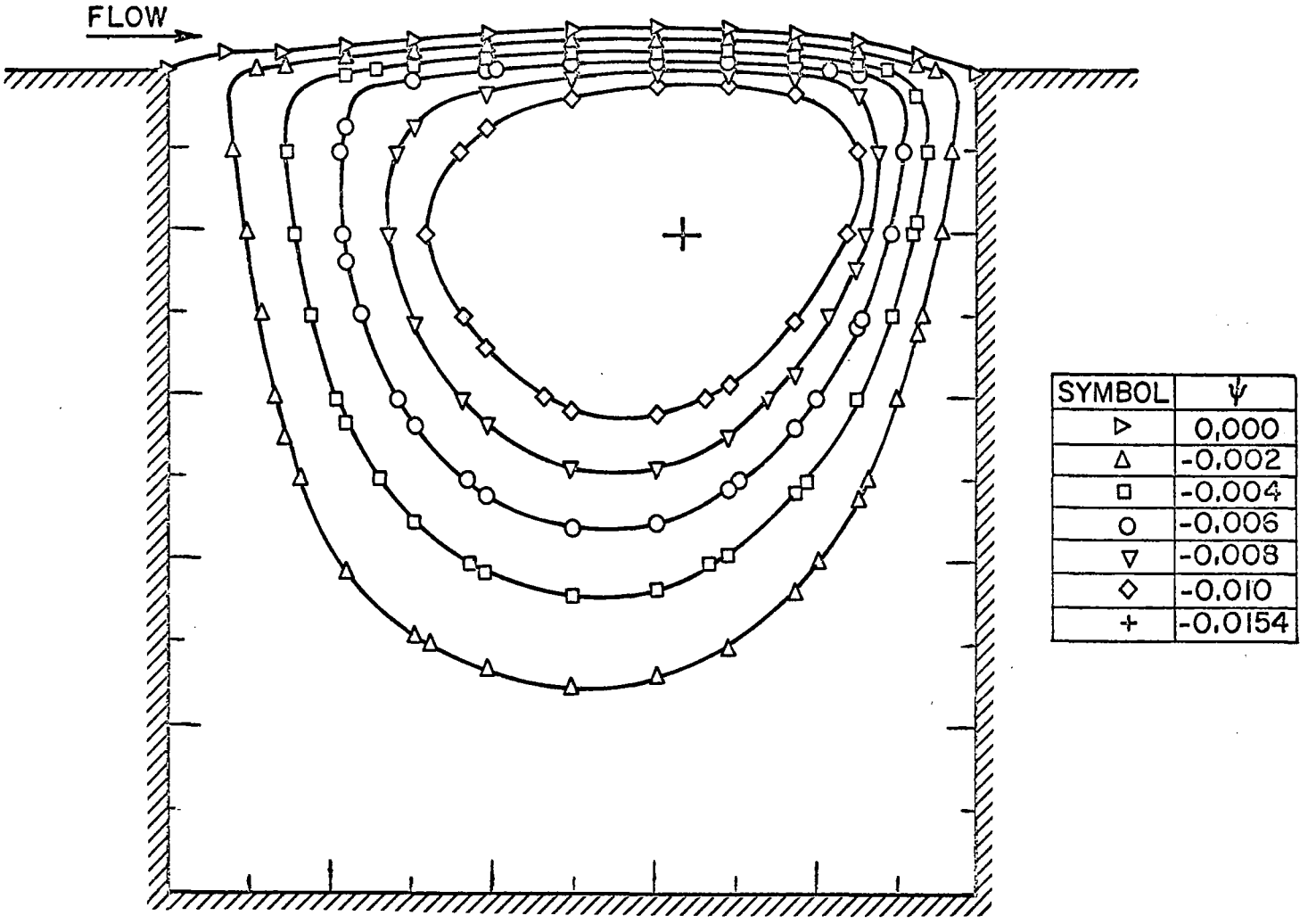

FIGURE 10. CONSTANT STREAMLINE CONTOURS. N_{Re}'=500.0, ASPECT RATIO=1.0.

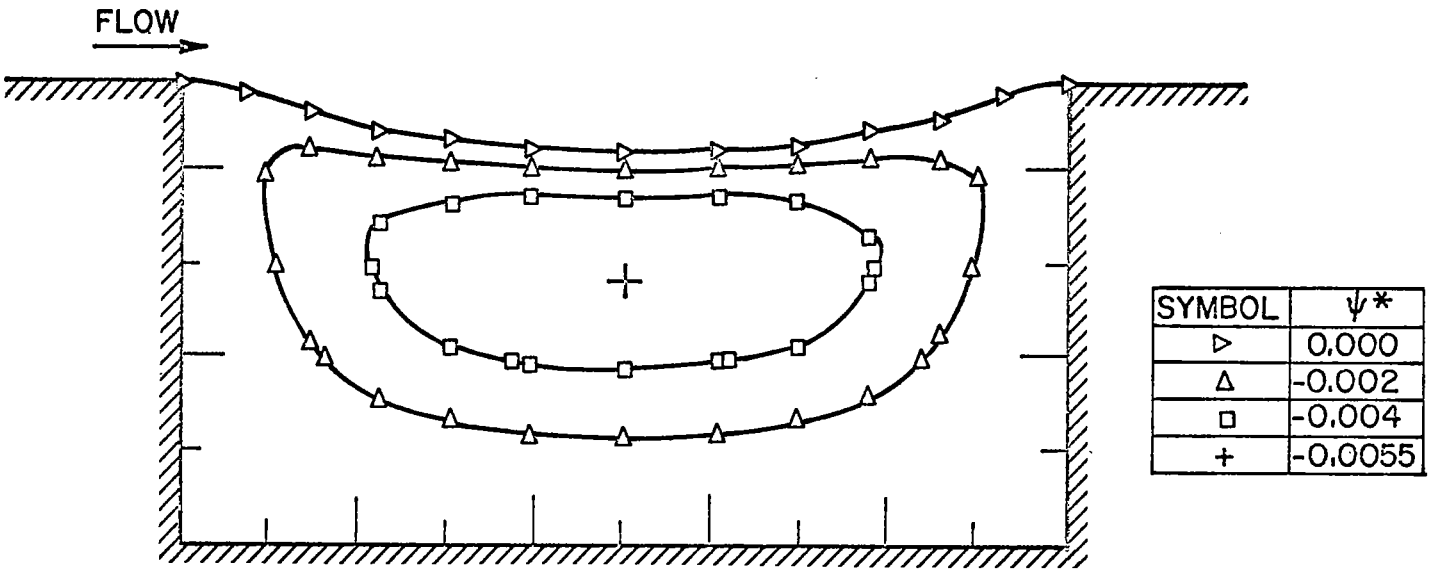

FIGURE 11. CONSTANT STREAMLINE CONTOURS, $N_{Re}' = 1.0$, ASPECT RATIO = 0.5.

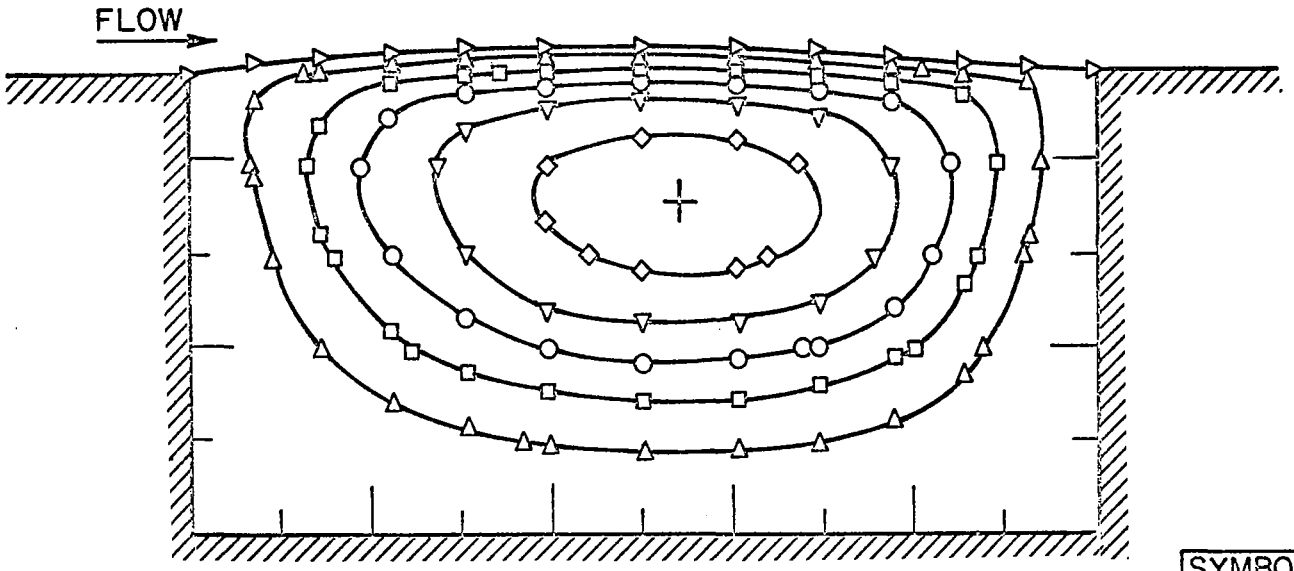

SYMBOL	ψ^*
▷	0.000
△	-0.002
□	-0.004
○	-0.006
▽	-0.008
◇	-0.010
+	-0.0109

FIGURE 12. CONSTANT STREAMLINE CONTOURS. $N_{Re}{}' = 100.0$, ASPECT RATIO = 0.5.

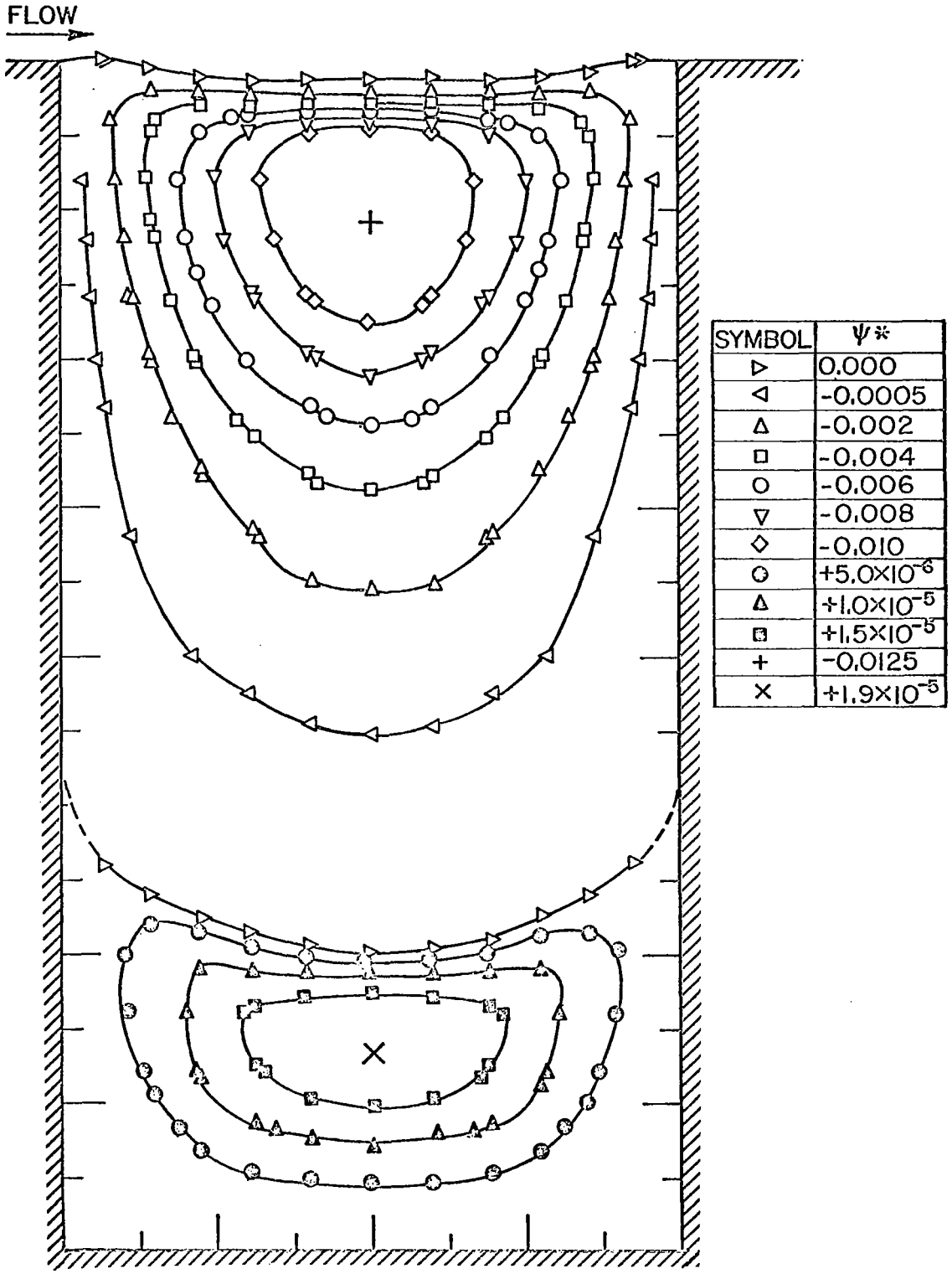

FIGURE 13. CONSTANT STREAMLINE CONTOURS.
$N_{Re}' = 1.0$, ASPECT RATIO = 2.0.

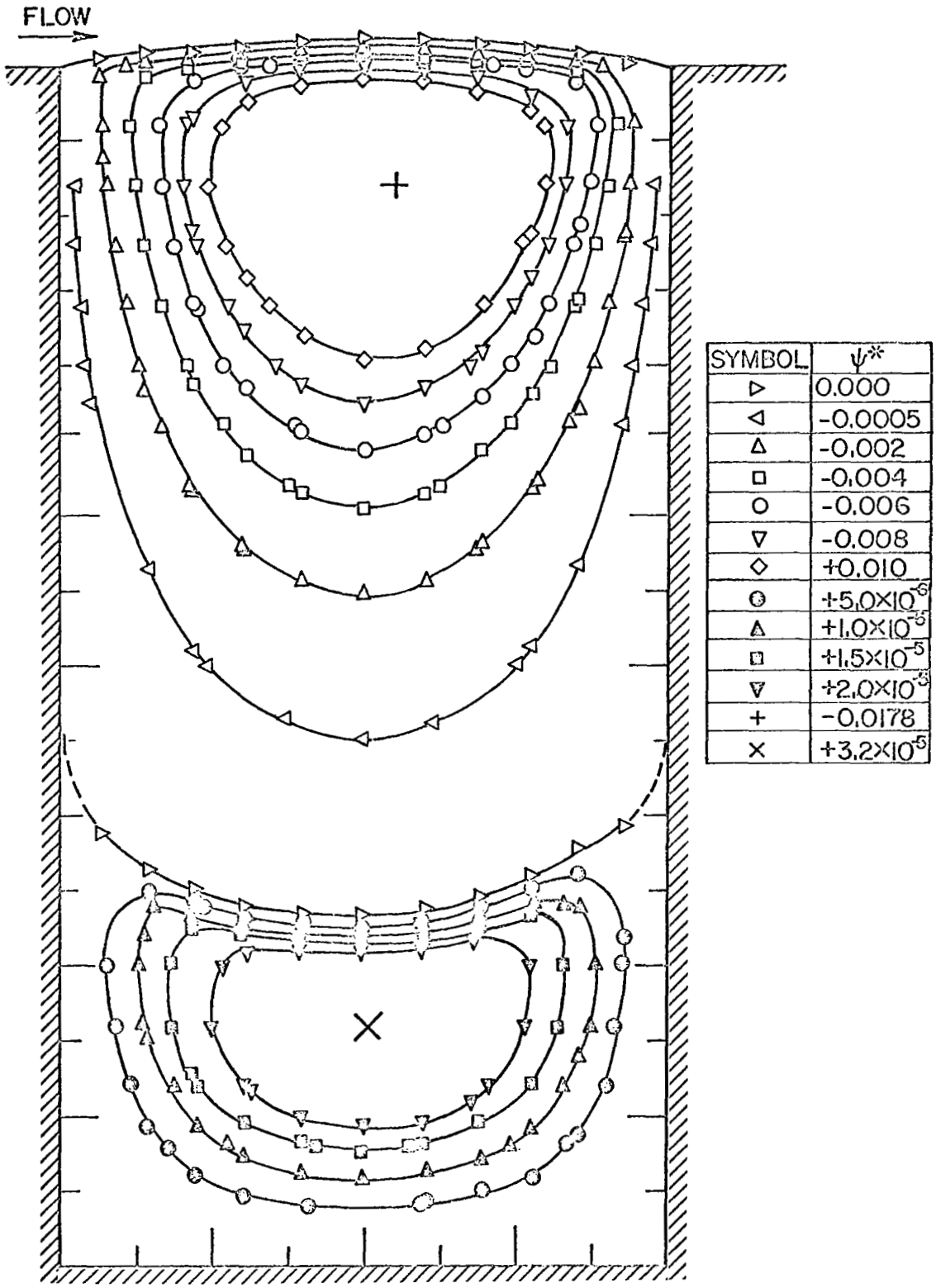

FIGURE 14. CONSTANT STREAMLINE CONTOURS. $N_{Re}' = 100.0$, ASPECT RATIO = 2.0.

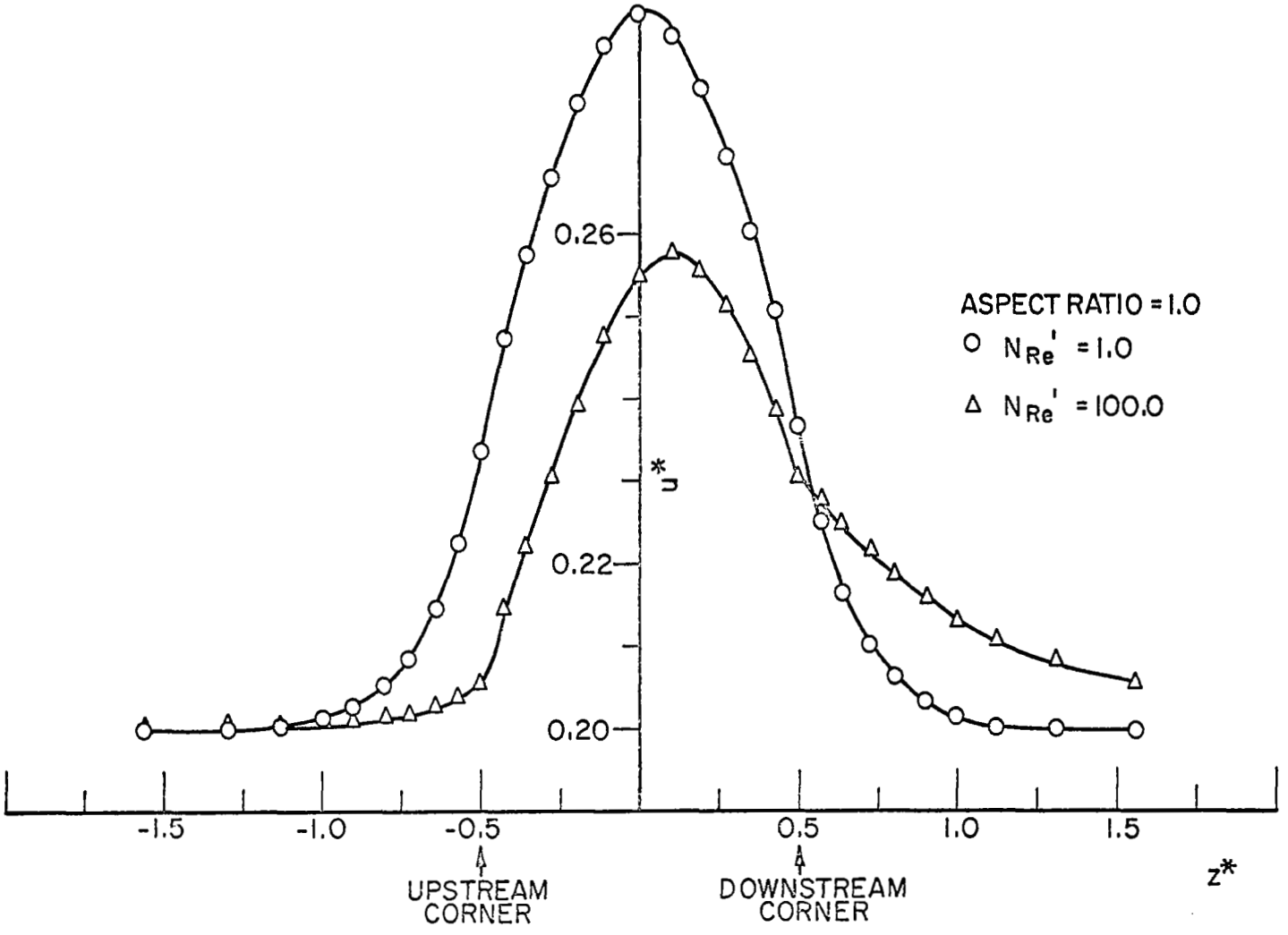

FIGURE 15. VARIATION OF u^* WITH RESPECT TO z^* AT $y^* = 0.9H^*$.

high Reynolds number the velocity in the neighborhood of the cavity deviates less from the corresponding value of the Couette flow at the entrance and the exit of the channel. The sudden removal of the presence of the channel wall results in a smaller acceleration of the particles next to the wall at high Reynolds numbers.

In the numerical procedure followed here, the upstream and downstream corner points (that may be singular) were considered to be grid points. The behavior of the solution at these points was therefore studied. Figs. 16 and 17 show the effect of changing Δy^* and Δz^* on the values of the vorticity at the corners. These values increase as Δy^* decreases (Δz^* being held constant). However, at one grid point upstream of the upstream corner and one grid point downstream of the downstream corner, values of vorticity were practically unchanged. (Note, for $\Delta y^* = 0.05$, the stream function and vorticity were relaxed one order of magnitdue lower than those for the other values of Δy^*.) When Δz^* was decreased, keeping Δy^* constant, the vorticity values at the corners were practically constant. Thus, it seems that these points do not appreciably influence the flow field at a small but finite distance away.

The development of the vortex in time was studied using the configuration of the prototype problem for $N'_{Re} = 10.0$. It was decided not to solve for the transient solution inside the cavity in a channel wall in order to concentrate only on the formation of the vortex and keep the computer cost low. The upper horizontal plate was moved with a constant velocity at $t^* > 0$. The nature of the vortex is shown in Figs. 18 to 23 for different t^*. The strength of the vortex increases uniformly and attains the steady-state value asymptotically (Fig. 24). This value is in better agreement with the value obtained by Burggraf than that calculated from steady-state equations. This

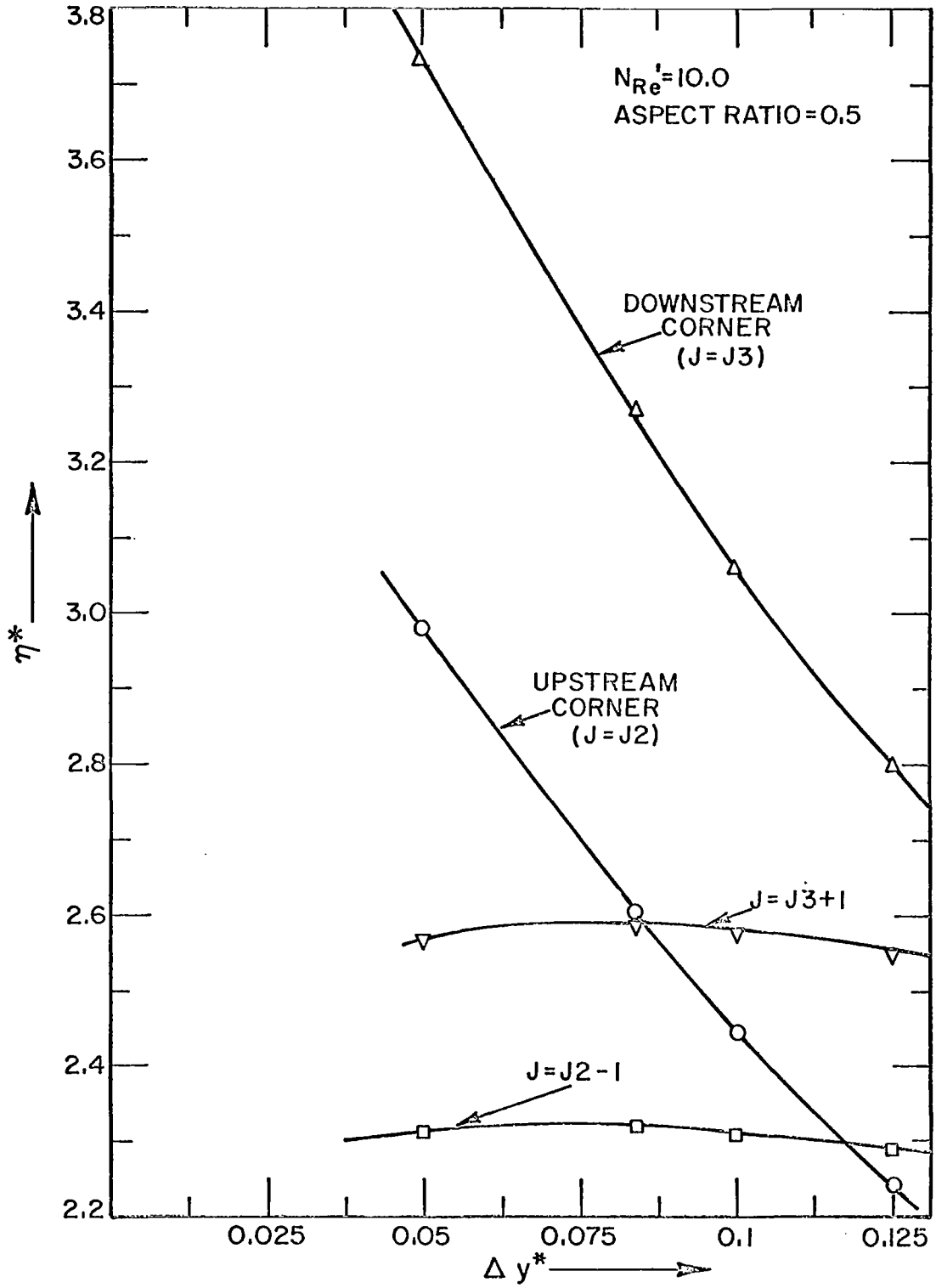

FIGURE 16. EFFECT OF CHANGING Δy^* ON VORTICITY AT CORNERS.

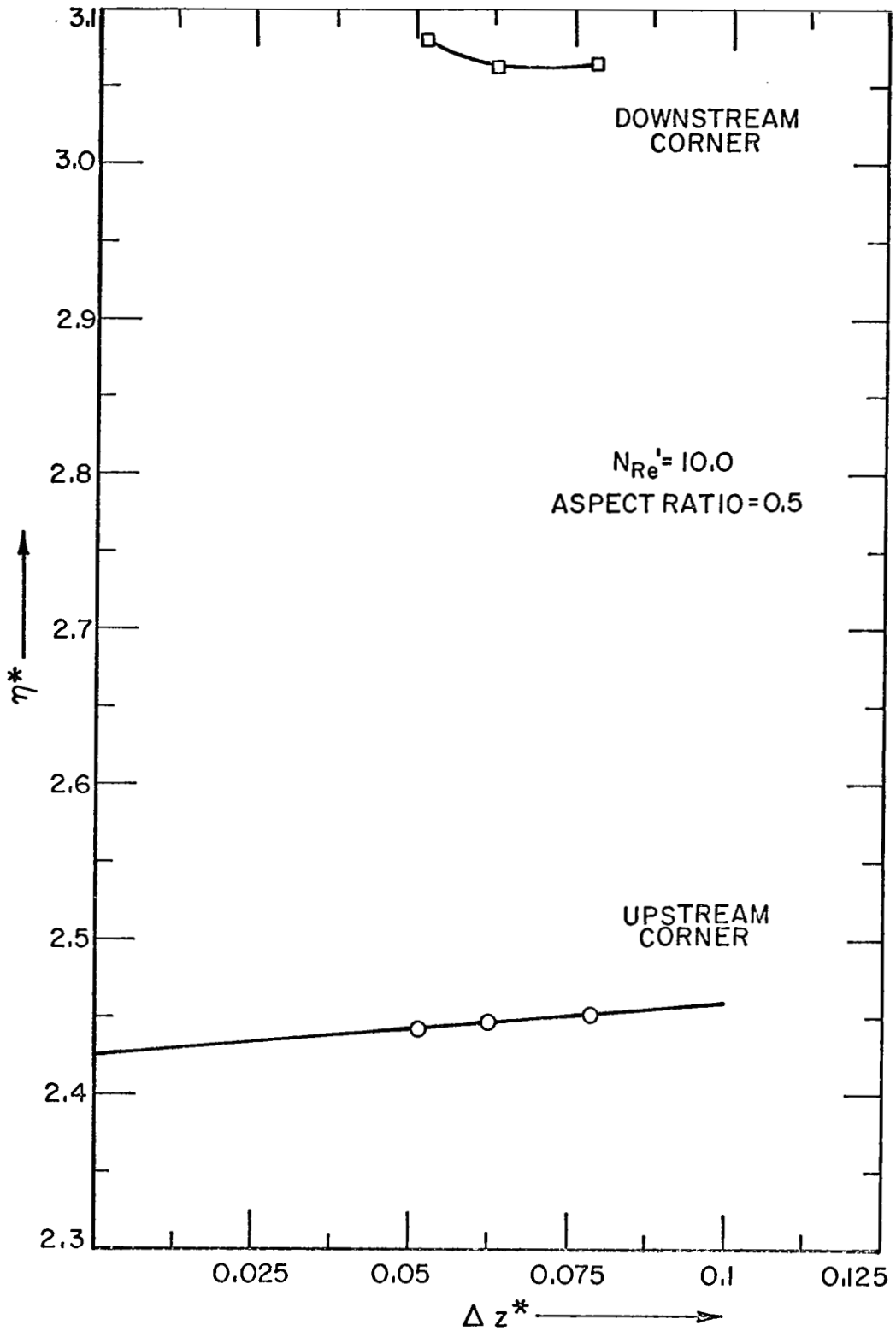

FIGURE 17. EFFECT OF CHANGING Δz^* ON VORTICITY AT CORNERS.

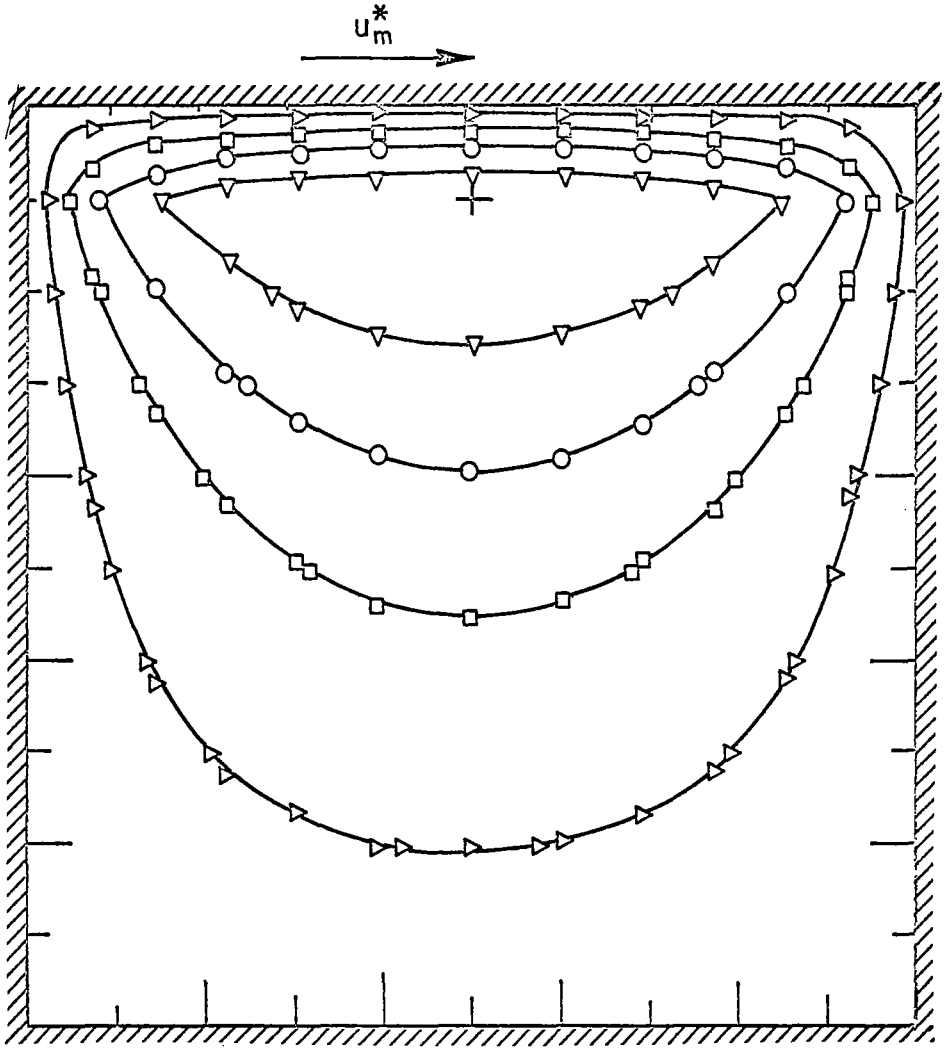

SYMBOL	ψ^*
▷	-0.004
□	-0.012
○	-0.02
▽	-0.03
+	-0.0417

FIGURE 18. CONSTANT STREAMLINE CONTOURS. $N_{Re}' = 10.0$, ASPECT RATIO=1.0, $t^* = 0.02$.

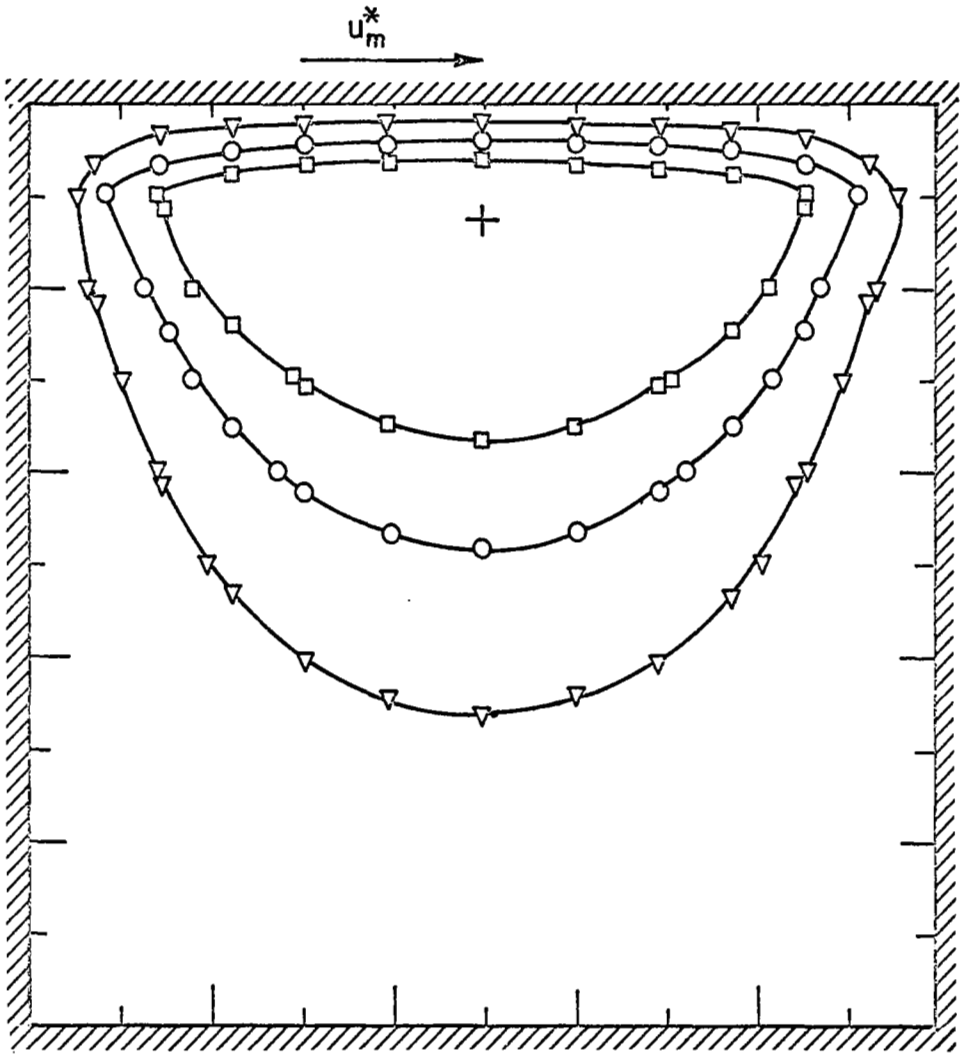

SYMBOL	ψ^*
▽	-0.02
○	-0.04
□	-0.06
+	-0.0975

FIGURE 19. CONSTANT STREAMLINE CONTOURS. $N_{Re}' = 10.0$. ASPECT RATIO = 1.0, $t^* = 0.06$.

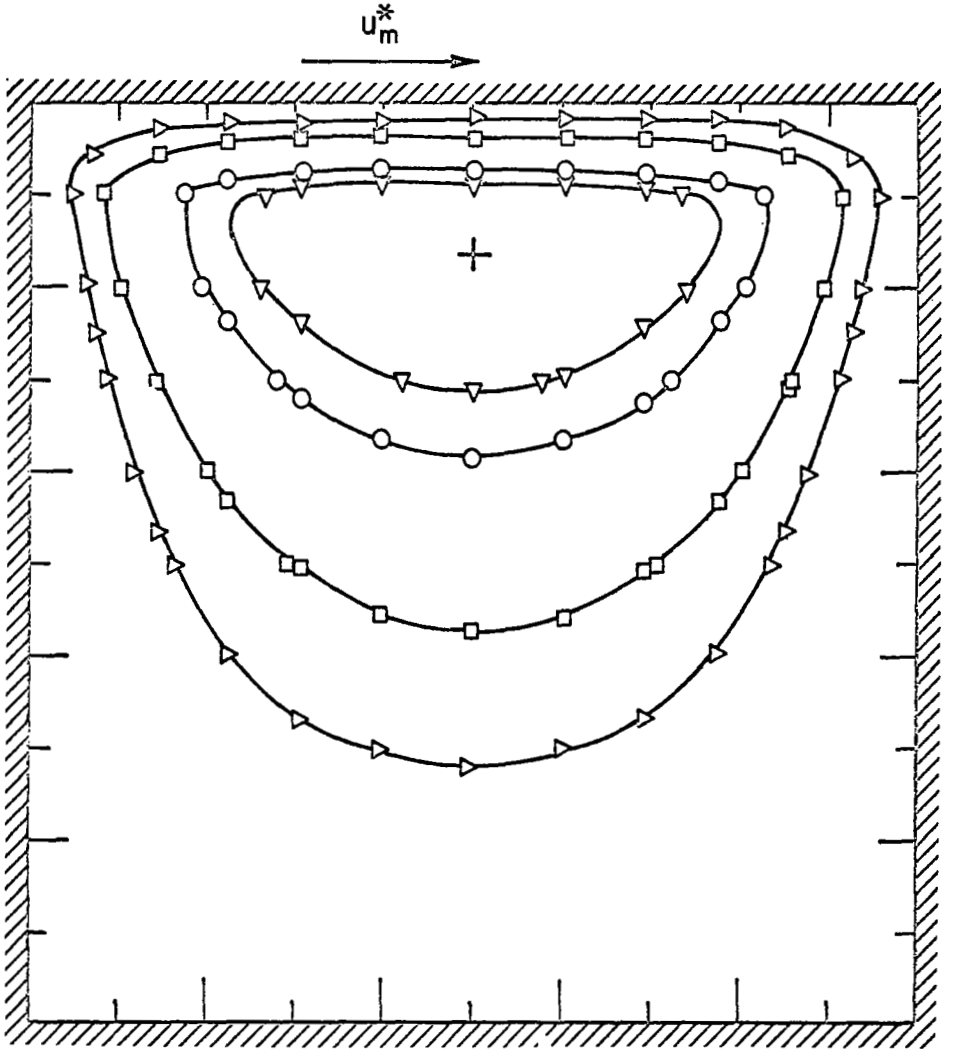

SYMBOL	ψ^*
▷	-0.02
□	-0.04
○	-0.08
▽	-0.10
+	-0.128

FIGURE 20. CONSTANT STREAMLINE CONTOURS, $N_{Re}' = 10.0$, ASPECT RATIO=1.0, $t^* = 0.1$.

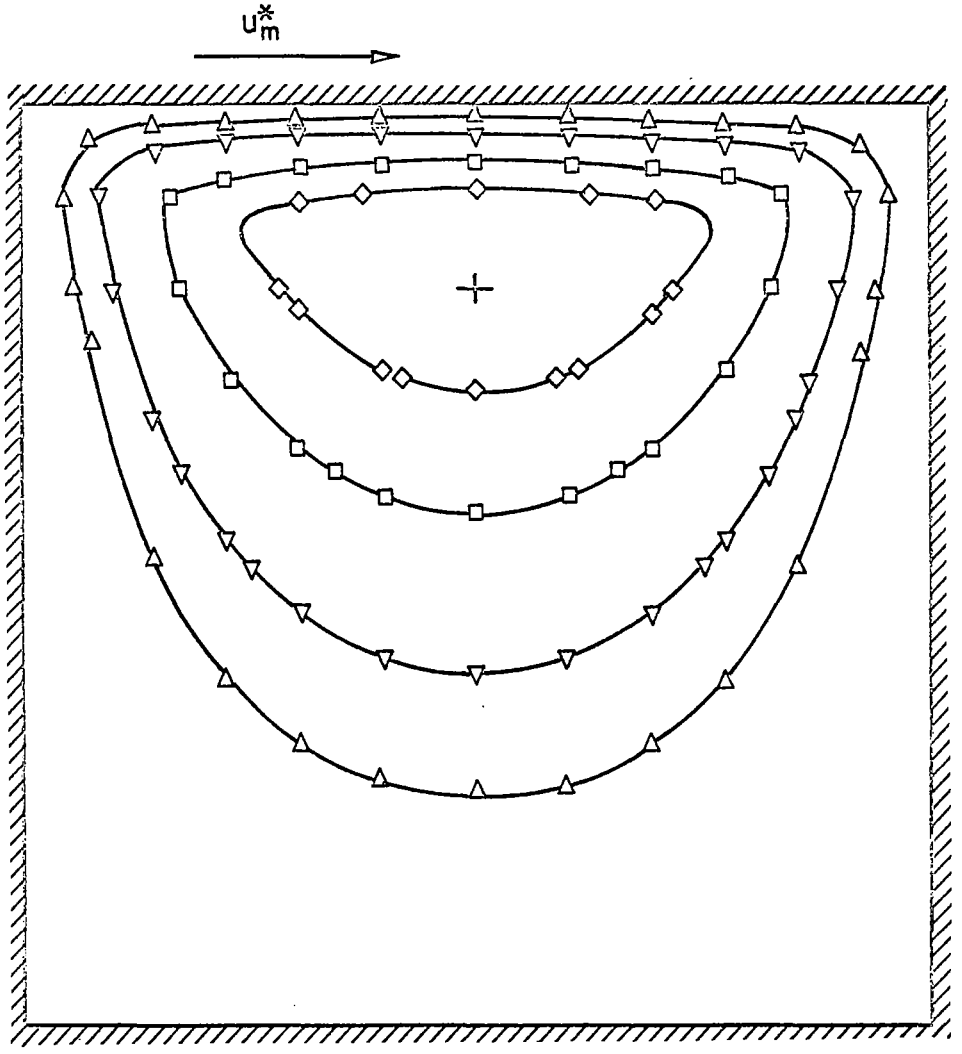

SYMBOL	ψ^*
△	-0.02
▽	-0.04
□	-0.08
◇	-0.12
+	-0.1467

FIGURE 21. CONSTANT STREAMLINE CONTOURS, $N_{Re}' = 10.0$, ASPECT RATIO=1.0, $t^* = 0.14$.

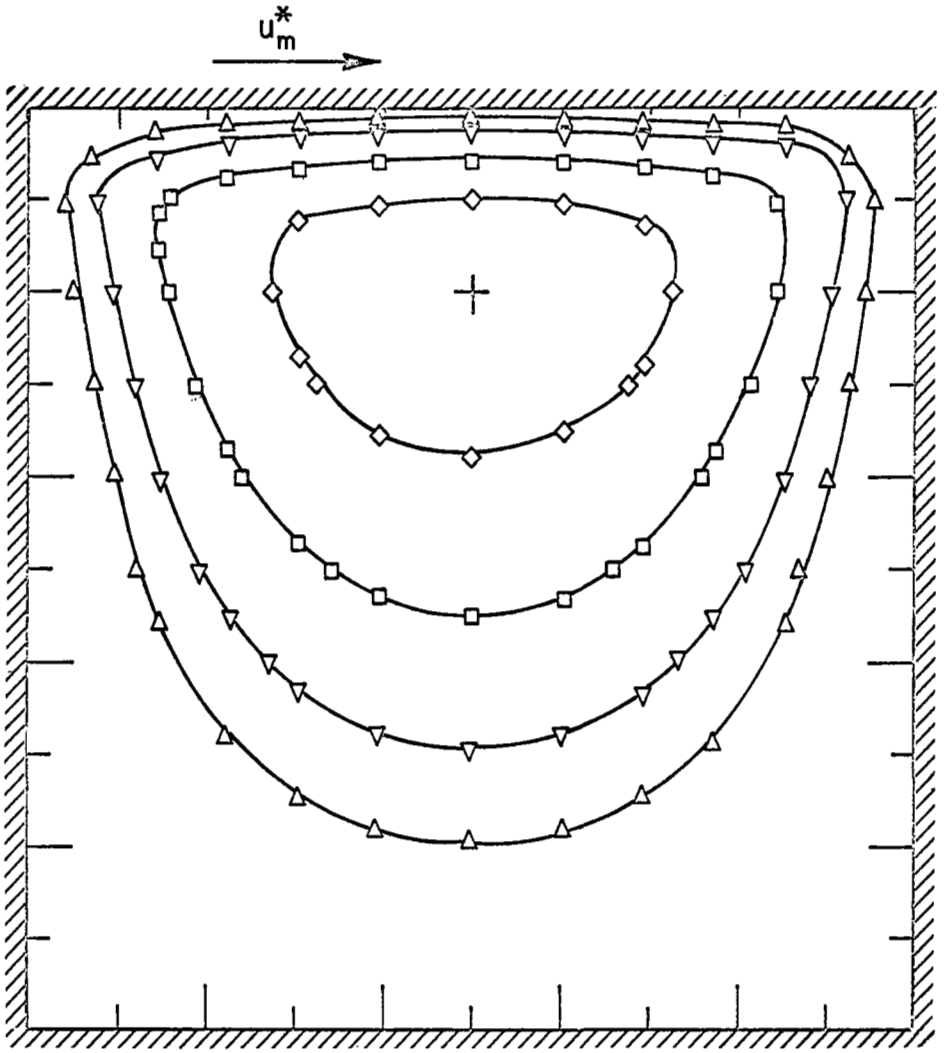

SYMBOL	ψ^*
△	-0.02
▽	-0.04
□	-0.08
◇	-0.12
+	-0.181

FIGURE 22. CONSTANT STREAMLINE CONTOURS. $N_{Re}' = 10.0$, ASPECT RATIO=1.0, $t^* = 0.31$.

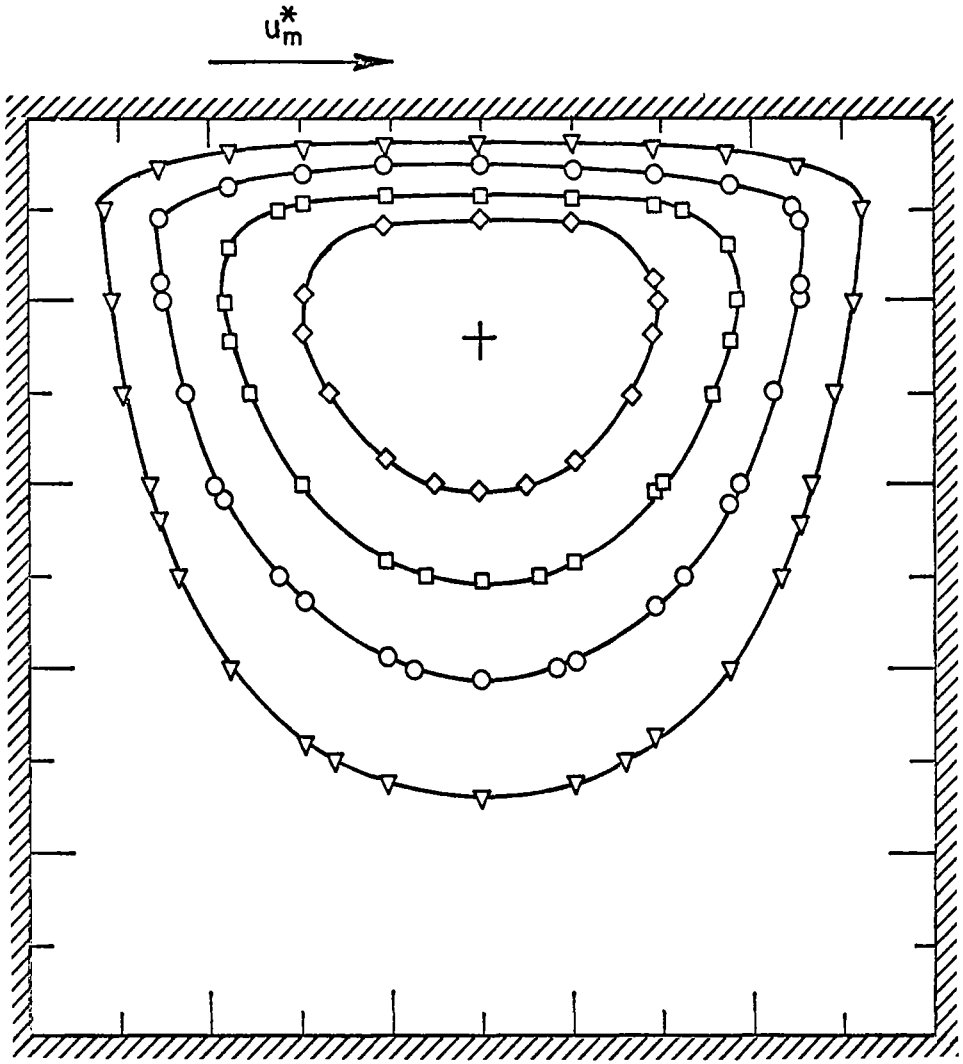

SYMBOL	ψ^*
▽	-0.04
○	-0.08
□	-0.12
◇	-0.16
+	-0.1972

FIGURE 23. CONSTANT STREAMLINE CONTOURS. $N_{Re}{}' = 10.0$, ASPECT RATIO = 1.0, $t^* = 0.78$.

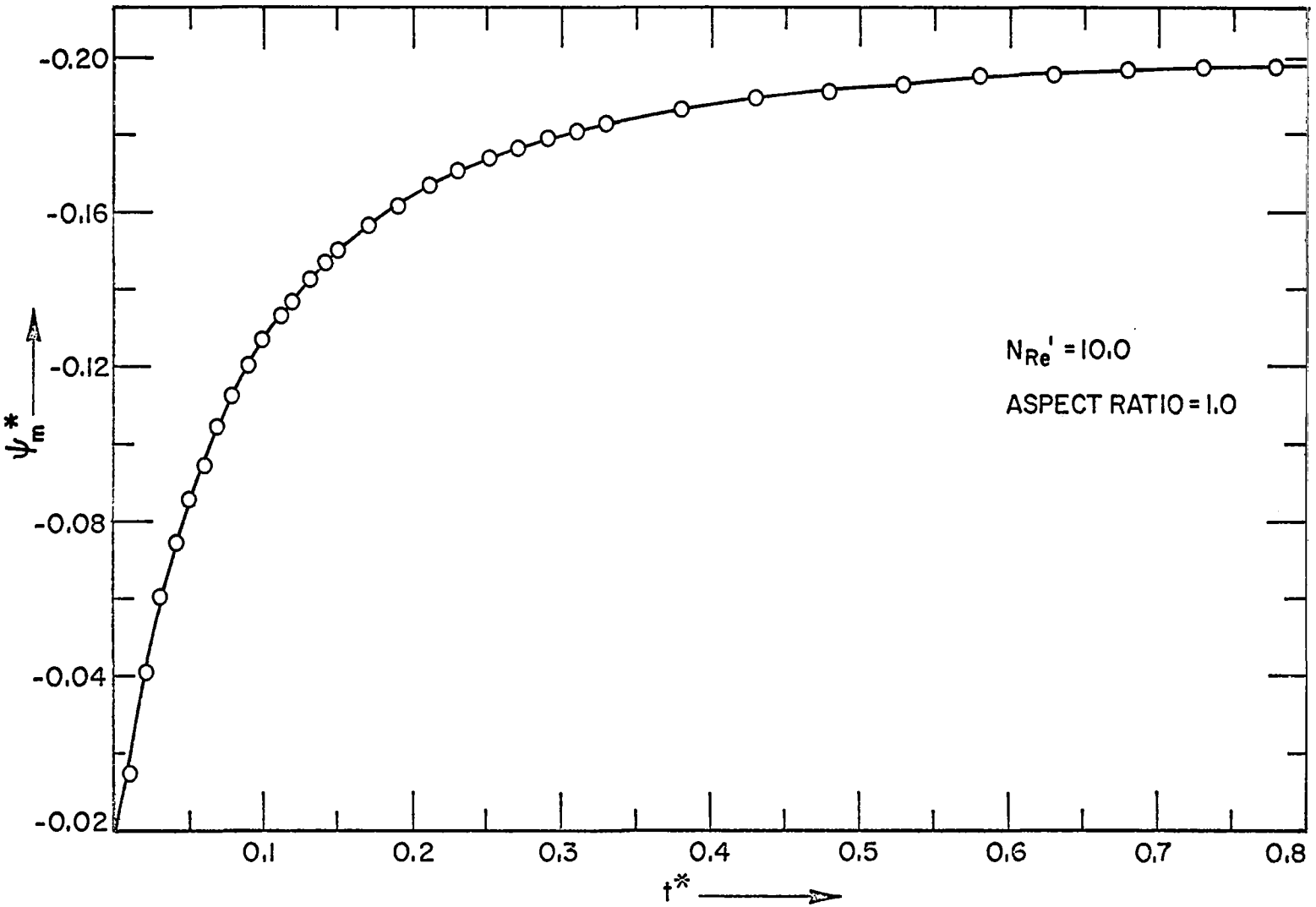

FIGURE 24. VORTEX DEVELOPMENT. $N_{Re}' = 10.0$, ASPECT RATIO = 1.0.

is mainly due to the fact that the unsteady-state finite difference formulation uses central differences whereas the steady-state formulation employs one-sided differences for first derivatives in the vorticity equation.

Finally, other investigators have reported corner eddies for square cavities. The present study that utilizes a relatively coarse grid does not indicate any corner eddies.

CHAPTER IV
CONCLUSIONS

1. Steady laminar incompressible flow in two-dimensional channels with a rectangular cut-out were obtained using an explicit numerical method for solving the complete Navier-Stokes equations. Solutions were obtained for aspect ratios of 0.5, 1.0 and 2.0, and for Reynolds numbers of 1, 10, 100, and 500.

2. The number of eddies present in the cavity depend only on the aspect ratio. For aspect ratios of 0.5 and 1.0, one vortex was observed. However, for aspect ratio of 2.0 two vortices were present, one on top of the other. The dividing streamline was at a cavity depth of 0.75 at Reynolds number unity and .709 at $N'_{Re} = 100$.

3. The streamline dividing the external flow and the cavity flow was concave for low Reynolds numbers and convex for high Reynolds numbers.

4. As the Reynolds number was increased, the strength of the vortex increased and then decreased, and the vortex center moved downstream and upward, creating a thin shear layer.

5. The calculated vorticity values at the upstream and downstream corners did not appear to approach a limit as the grid size was decreased. However, the vorticity values at nodal points next to these corners, leveled off as the number of grid points was increased.

6. In the present problem the shear layer on top of the cavity and along the cavity wall is not very thin even at large Reynolds number (based on channel flow) hence, results obtained with relatively coarse grid may be accurate even at large Reynolds numbers.

7. In order to observe the actual vortex formation the time-dependent solution for the prototype problem was determined using an implicit alter-

nating direction method to solve the vorticity equation and an explicit relaxation procedure for the solution of the stream function equation. The strength of the vortex increased uniformly and attained the steady state value asymptotically.

8. The steady-state results determined from the unsteady-state equations were in better agreement with Burggraf's results (for the prototype problem) than those calculated from steady-state equations. This may be due mainly to the fact that in the former study central differences were used for first derivatives whereas one-sided differences were used in the latter study.

APPENDIX
THE FORTRAN PROGRAM

In this appendix the computer program used in this work is briefly described. The program was written in Fortran IV for the IBM 360 Computer. The notations used in the program are listed and defined below.

Fortran Symbol	Explanation
IC	Last grid point in the y^*-direction of the channel
IL	Last grid point in the y^*-direction (channel plus cavity)
JL	Last grid point in x^*-direction
NMAX	Maximum number of iterations for ψ^* and steady-state η^* equations
KL1	Frequency of print-out of maximum residues
KL2	Output option: 1 - no CHRT output
KL3	Output option: 5 - read ψ^*, η^*, u^*, v^* and t^* from magnetic tape, 6 - write ψ^*, η^*, u^*, v^* and t^* on magnetic tape, 7 - do both of above
KL4	Problem option: 1 - prototype problem, 2 - channel with cavity
KL5	Output option: 1 - no ψ^* and η^* CHRT output
KL6	Plane option: 1 - no transformation, 3 - transformed plane
KL9	Frequency of unsteady-state CHRT output
KL10	State option: 1 - unsteady state
KL13	Initial value option: 1 - initial values printed
KL14	u, v, x and y printed (dimensional output)
KL16	Nature of boundary condition at J = JL: 1 - functions ψ^* and η^* defined, otherwise normal derivatives equal to zero

KL18	Must be equal to 1
C	$\Delta x^*/\Delta y^*$
RNN	Reynolds number, N'_{Re}
BPSI	Over-relaxation factor for stream function equation
BVRT	Must be equal to 1
DPSIM	Maximum allowable residue of ψ^*
DVRTM	Maximum allowable residue of η^* (for steady-state)
J2	Value of J at which the cavity starts
JM	Value of J about which the cavity is symmetric
J3	Value of J at which the cavity ends
LENGTH	Dimensional length of the cavity
DLTT	Δt^*
NTMAX	Number of time steps
NMAX1	Maximum number of iterations for ψ^* (unsteady state)
ZMIN	Must be 0.5
KL0, KL7, KL15, KL19, KL20, KL21, HL, ZMAX, AA	Dummy variables - not used in the program
U	The velocity in y^*-direction
W	The velocity in x^*-direction
PSI	ψ^*
VRT	η^*
DIST	x^*
Y	y^*
DLTZ	Δz^*
DLTY	Δy^*

Note, during the utilization of the computer program given here, the comments listed in the main program and the ones listed below should be kept in mind.

1. Height of the channel and the length of the cavity should be the same.

2. Do not use transformations given by the options KL6 = 2 and KL6 = 4.

3. The prototype problem can be solved only for aspect ratio of 1.0.

4. The present form of the program is not capable of solving for the transient solution of the flow in the channel having a cavity.

```
// EXEC FORTRAN
C
C       CR (OR CZ) POS.-BACK.DER.   CR (OR CZ)NEG.- FORW. DER)            1PF00020
C
       COMMON ICMN,IC,ICPL,ILMN,IL,ILPL,JLMN,JL,JLPL,KL0,KL1,KL3,KL4,KL5,
      1KL7,KL13,KL14,KL15,KL16,KL19,KL20,C,BPSI,BVRT,DPSIM,
      2RNN,DTZ2,DT2Y,Z(60),B,CWC,SVRCF,YTRN(40),Y(40),YSQ(40),
      3YT1(40),YTSQ(40),YT2(40),ZT1(60),ZTSQ(60),ZT2(60),
      4DIST(60),PSI(40,60),VRT(40,60),U(40,60),W(40,60),LN,
      5PSIMAX,ITV,JTV,DPSILD,DVRTLD,DLTY,DLTZ,JLB,ITS,JTS,
      6JLBPL,J2,JMMN,JM,JMPL,J3,P(40,60),EL,LENGTH,LNUN,NT,
      7A1(60),A2(40),A3(60),A4(40),DLTT,KL10,NMAX1,WMAX,TIME
       REAL LENGTH
     1 READ(1,200) IC,IL,JL,NMAX,KL0,KL1,KL2,KL3,KL4,KL5,KL7,KL9,KL10,
      1KL13,KL14,KL15,KL16,KL19,KL20,C,RNN,BPSI,
      2BVRT,DPSIM,DVRTM,J2,JM,J3,TIME,LENGTH,DLTT,NTMAX,NMAX1
   200 FORMAT(16I5,/3I5,4F10.5,/,2E10.2,3I5,3F10.5,2I5)
C
C       IF KL4=1, KL0=JL+20
C       IF KL4=2, KL0=JL
C       IF KL4=1,GIVE J2,JM AND J3. JM=KL0/2+1. J3-J2=JL-2. JM-J2=J3-JM
C       KL4 SHOULD BE EITHER 1 OR 2
C       C=(IC-1)/(KL0/2-1)
C       KL1 - FREQUENCY OF PRINT-OUT OF MAXIMUM RESIDUE FOR STEADY STATE
C       IF KL2=1, NO CHRT OUTPUT
C       IF KL3=1, PUNCHED OUTPUT
C       IF KL4=1, CONSTANT CROSS-SECTION AND IC=IL
C       IF KL4=1, KL6=1 AND KL16=1
C       IF KL4=2 CAVITY PROBLEM
C       IF KL4.NE.1, DLTY AND HENCE C DEFINED ON Y(IC)
C       IF KL5=1, NO STREAM FUNCTION AND VORTICITY OUTPUT
C       IF KL6 GT 1 CALCULATIONS WITH TRANSFORMATION
C       IF KL6=2, TRUNCATED ARCTANGENT TRANSFORMATION -
C       X=(ARCTAN(A*Z)-ARCTAN(A*ZMIN))/(PAI/2.0-ARC(A*ZMIN))
C       IF KL6=2, GIVE ZMIN AND X
```

```
C     IF KL6=4, ARCTANGENT TRANSFORMATION-X=0.5*(1.0+2.0/PAI*ARCTAN(A*Z))
C     IN Z-DIRECTION
C     IF KL10=1, UNSTEADY STATE
C     IF KL13.EQ.1, INITIAL VALUES OF PSI,VRT,U,W AND V ARE PRINTED
C     IF KL14=1, U,V AND W IN DIMENSIONAL FORM
C     IF AA.NE.0.0, Z(JL)=1.0 AND KL6.GT.1 -THE LAST POINT IN
C     Z-DIRECTION CONSIDERED AT INFINITY
C     IF KL16=1, THEN FUNCTIONS DEFINED AT AT J=JL
C     IF KL16.NE.1, NORMAL DERIVATIVE OF VORTICITY AND STREAM FUNCTION ZERO
C     AT J=JL. USE IT FOR KL4=2 ONLY
C     IF KL18=1, NO TRANSFORMATION IN Y-DIRECTION
C     J=J2 CAVITY STARTS
C     J=J3 CAVITY ENDS
C     IF KL4=2, GIVE J2 AND J3
C
      WRITE(3,205)IC,IL,JL,NMAX,KL0,KL1,KL2,KL3,KL4,KL5,KL7,KL9,KL10,
     1KL13,KL14,KL15,KL16,KL19,KL20,C,RNN,BPSI,
     2BVRT,DPSIM,DVRTM,J2,JM,J3,TIME,LENGTH,DLTT,NTMAX,NMAX1
  205 FORMAT(1H1,//,3X,7HIC    =I3,3X7HIL    =I3,3X7HJL    =I3,3X7HNMAX
     1 =I3,3X7HKL0   =I3,3X7HKL1   =I3,3X7HKL2   =I3,3X7HKL3   =I3,3X7HK
     2L4   =I3,3X7HKL5   =I3,//          ,3X7HKL7   =I3,3X7HKL9   =I3,
     3 3X7HKL10  =I3,3X7HKL13  =I3,3X7HKL14  =I3,3X7HKL15  =I3,
     4     3X7HKL16  =I3,3X7HKL19  =I3,3X7HKL20  =I3//,3X,7HC     =
     51PE12.5,//,3X7HRNN   =1PE12.5,3X7HBPSI  =1PE12.5,3X,
     67HBVRT  =1PE12.5,//,3X7HDPSIM =1PE12.5,3X
     7                  7HDVRTM =1PE12.5,3X7HJ2    =I3,3X7HJM    =I3,
     83X7HJ3    =I3,3X7HHL    =E12.5,3X7HLENGTH=E12.5//3X7HDLTT  =E12.5,
     93X7HNTMAX =I3,3X7HNMAX1 =I3)
      JMMN=JM-1
      JMPL=JM+1
      JLMN=JL-1
      JLPL=JL+1                                                    1PF00820
      ILMN=IL-1                                                    1PF00830
      ILPL=IL+1                                                    1PF00840
      ICMN=IC-1
      ICPL=IC+1
```

```
      JLB=JL
      JLBPL=JLPL
      DO  5 J=1,JLPL
      DO  5 I=1,ILPL
      PSI(I,J)=0.0
      VRT(I,J)=0.0
        U(I,J)=0.0
    5   W(I,J)=0.0
      DPSILD=0.0
      DVRTLD=0.0
      NT=0
      LNUN=0
      LN=0
      CALL SETUP                                                    1PF00230
C     IF KL3=5 READ  PSI, VRT,U, W AND TIME ON UNIT 08
C     IF KL3=6 WRITE PSI, VRT,U, W AND TIME ON UNIT 10
C     IF KL3=7 DO BOTH OF ABOVE
      IF (KL3-5) 301, 302, 301
  301 IF (KL3-7) 303, 302, 303
  302 REWIND 8
      READ (8)      (( PSI(I,J),I=1,IL), J=1,JL),
     1              (( VRT(I,J),I=1,IL), J=1,JL) ,
     2              ((   W(I,J),I=1,IL), J=1,JL),
     3              ((   U(I,J),I=1,IL), J=1,JL),TIME
      REWIND 8
  303 CONTINUE
      IF ((KL13)-(1)) 6,31001,6                                     ))CASA>>
31001 CALL CHRT
    6 CONTINUE
      IF (KL10-1) 7,15,7
C
C     STEADY STATE CALCULATIONS
C
    7 DO 10 N=1,NMAX
      LN=N                                                          1PF00500
      CALL STREET                                                   1PF00510
```

```
      IF ((ABS(DPSILD))-(1.E10)) 31002,31002,14
31002 CALL BCUND
      CALL VORTCT
      IF(LN-(LN/KL1)*KL1) 9,8,9
    8 WRITE(3,210) LN,ITS,JTS,DPSILD,ITV,JTV,DVRTLD
  210 FORMAT(1H0,3X,3HLN=I4,5X,7HDPSILD(I2,1H,I2,2H)=1PE12.5,5X,
     1                      7HDVRTLD(I2,1H,I2,2H)=1PE12.5)
    9 IF (DPSIM-ABS(DPSILD)) 10,10,1000
 1000 IF (DVRTM-ABS(DVRTLD)) 10,10,11
   10 CONTINUE
   11 IF(LN-(LN/KL1)*KL1) 12,13,12
   12 WRITE(3,210) LN,ITS,JTS,DPSILD,ITV,JTV,DVRTLD
   13 IF ((KL2)-(1)) 14,1,14                                    ))CASA>>
   14 CALL CHRT
      GO TO 1
C
C     UNSTEADY STATE CALCULATIONS
C
   15 NTIN=1
      NTFL=NTMAX
      IF (KL3-5) 30,26,25
   25 IF (KL3-7) 30,26,30
   26 NTIN=2
      NTFL=NTMAX+1
   30 DO 20 NT=NTIN,NTFL
      TIME=TIME+DLTT
      CALL BCUND
      CALL ACI
      CALL STRFCT
      WRITE(3,220) LNUN,ITS,JTS,DPSILD
  220 FORMAT(//3X,7HLNUN  =I3,3X7HDPSILD(I2,1H,I2,2H)=1PE12.5)
      IF (LNUN-NMAX1) 17,17,21
   17 IF (NT-(NT/KL9)*KL9) 20,18,20
   18 CALL CHRT
      WRITE(3,225) TIME
  225 FORMAT(//3X7HTIME  =1PE12.5)
```

```
   20 CONTINUE
      GO TC 1
   21 CALL CHRT
      GO TO 1
      END                                                              1PF00730
// EXEC FORTRAN
      SUBROUTINE SETUP
      COMMON ICMN,IC,ICPL,ILMN,IL,ILPL,JLMN,JL,JLPL,KL0,KL1,KL3,KL4,KL5,
     1KL7,KL13,KL14,KL15,KL16,KL19,KL20,C,BPSI,BVRT,DPSIM,
     2RNN,DTZ2,DT2Y,Z(60),B,CWC,SVRCF,YTRN(40),Y(40),YSQ(40),
     3YT1(40),YTSQ(40),YT2(40),ZT1(60),ZTSQ(60),ZT2(60),
     4DIST(60),PSI(40,60),VRT(40,60),U(40,60),W(40,60),LN,
     5PSIMAX,ITV,JTV,DPSILD,DVRTLD,DLTY,DLTZ,JLB,ITS,JTS,
     6JLBPL,J2,JMMN,JM,JMPL,J3,P(40,60),HL,LENGTH,LNUN,NT,
     7A1(60),A2(40),A3(60),A4(40),DLTT,KL10,NMAX1,WMAX,TIME
      REAL LENGTH
       DLTY=1./ FLOAT(ICMN)
        DLTZ=DLTY*C
       DTZ2=DLTZ*DLTZ
      DO 5  J=1,KL0
    5  Z(J)=DLTZ*FLOAT(J-2)
      B=1./C**2                                                        1PF00870
      DT2Y=DLTY*DLTY
      CWC=2.0/DT2Y
      DO 10 I=1,IL
   10 YTRN(I)=DLTY*(FLOAT(I)-1.0)
      READ(1,200) ZMAX,KL6,KL18,KL20,KL21,AA,ZMIN
  200 FORMAT(F10.5,4I5,2F10.5)
      WRITE(3,205)ZMAX,KL6,KL18,KL20,KL21,AA,ZMIN
  205 FORMAT(/3X7HZMAX  =1PE12.5,3X7HKL6   =I3,3X7HKL18  =I3,3X7HKL20  =
     1I3,3X           7HKL21  =I3,3X7HAA    =E12.5, 3X7HZMIN  =E12.5)
      IF ((KL16)-(1)) 31005,31006,31005                                ))CASA>>
31006 JLBPL=JLMN                                                       ))CASA>>
31005 IF ((KL16)-(1)) 31007,31008,31007                                ))CASA>>
31008 JLB=JLMN                                                         ))CASA>>
31007 CONTINUE                                                         ))CASA>>
```

```
C
C      WMAX AND LENGTH SHCULD BE DIMENSIONAL
C
       READ(1,222) WMAX
  222  FORMAT(F10.5)
       WRITE(3,225) WMAX
  225  FORMAT(/,3X7HWMAX  =1PE12.5)
       PSIMAX=WMAX*LENGTH*YTRN(IC)/2.0
       DO 70 J=2,JLB
   70  W(1,J)=WMAX*LENGTH/PSIMAX
       IF (KL10-1) 49,80,49
   49  IF (KL4-2) 80,50,80
   50  DO 71 J=2,JL
   71  PSI(1,J)=1.0
   80  CONTINUE
C
C      TRANSFORMATIONS USED IN RADIAL AND AXIAL DIRECTIONS
C
       PAI=3.141592654
       IF ((AA)-(0.0)) 9,31009,9                                          ))CASA>>
31009  GO TO (9,6,7,9), KL6
    6  TANINV=-Z(JM)*PAI/(2.0-2.0*Z(JM))
       AA=(SIN(TANINV)/COS(TANINV))/ZMIN
       GO TO 9
    7  AA=ALOG((1.0+(1.0-Z(J2))/Z(J2))/(1.0-(1.0-Z(J2))/Z(J2)))/2.0/0.5
    9  CONTINUE
       DO 15 I=1,IL
       GO TO (11,12), KL18
   11  Y(I)=YTRN(I)
       YT1(I)=1.0
       YT2(I)=0.0
       GO TO 14
   12  CONTINUE
   14  CONTINUE
       YTSQ(I)=YT1(I)*YT1(I)
       YSQ(I)=Y(I)*Y(I)
```

```
   15 CONTINUE
      DO 20 J=1,JL
      GO TO (16,17,18,170),KL6
   16 DIST(J)=Z(J)
      ZT1(J)=1.0
      ZT2(J)=0.0
      GO TO 19
   17 ARG=Z(J)*PAI/2.0+TANINV*(1.0-Z(J))
      DIST(J)=(SIN(ARG)/COS(ARG))/AA
      ZT1(J)=AA/((PAI/2.0-TANINV)*(1.0+(AA*DIST(J))**2))
      ZT2(J)=-AA*SIN(Z(J)*PAI+2.0*TANINV*(1.0-Z(J)))
      GO TO 19
  170 IF ((J)-(1)) 31011,20,31011                                    ))CASA>>
31011 IF ((J)-(JL)) 31010,20,31010                                   ))CASA>>
31010 ARG=PAI*(Z(J)-0.5)
      DIST(J)=(SIN(ARG)/COS(ARG))/AA
      ZT1(J)=AA/(PAI*(1.0+(AA*DIST(J))**2))
      ZT2(J)=-2.0*AA*PAI*DIST(J)*ZTSQ(J)
   19 ZTSQ(J)=ZT1(J)*ZT1(J)
   20 CONTINUE
      RETURN
   18 TANHA=1.0+TANH(0.5*AA)
      DO 30 J=3,JM
      ARG=Z(J)*TANHA-1.0
      DIST(J)=ALOG((1.0+ARG)/(1.0-ARG))/2.0/AA-0.5
      TANHZ=TANH(AA*(DIST(J)+0.5))
      ZT1(J)=AA*(1.0-TANHZ**2)/TANHA
      ZT2(J)=-2.0*AA*ZT1(J)*TANHZ
      ZTSQ(J)=ZT1(J)*ZT1(J)
      JD=KL0+1-J+1
      DIST(JD)=-DIST(J)
      ZT1(JD)= ZT1(J)
      ZT2(JD)=-ZT2(J)
   30 ZTSQ(JD)=ZTSQ(J)
      ZT1(2)=0.0
      ZT2(2)=0.0
```

```
      ZTSQ(2)=0.0
      ZT2(JM)=0.0
      ZT1(KL0)=0.0
      ZT2(KL0)=0.0
      ZTSQ(KL0)=0.0
      DIST(2)=0.0
      DIST(KL0)=0.0
      IF (KL4-2) 92,93,92
   92 J=1
      DO 94 JJ=J2,J3
      J=J+1
      DIST(J)=DIST(JJ)
      ZT1(J)=ZT1(JJ)
      ZTSQ(J)=ZTSQ(JJ)
   94 ZT2(J)=ZT2(JJ)
   93 RETURN
      END
// EXEC FORTRAN
      SUBROUTINE STRFCT
      COMMON ICMN,IC,ICPL,ILMN,IL,ILPL,JLMN,JL,JLPL,KL0,KL1,KL3,KL4,KL5,
     1KL7,KL13,KL14,KL15,KL16,KL19,KL20,C,BPSI,BVRT,DPSIM,
     2RNN,DT72,DT2Y,Z(60),B,CWC,SVRCF,YTRN(40),Y(40),YSQ(40),
     3YT1(40),YTSQ(40),YT2(40),ZT1(60),ZTSQ(60),ZT2(60),
     4DIST(60),PSI(40,60),VRT(40,60),U(40,60),W(40,60),LN,
     5PSIMAX,ITV,JTV,DPSILD,DVRTLD,DLTY,DLTZ,JLB,ITS,JTS,
     6JLBPL,J2,JMMN,JM,JMPL,J3,P(40,60),HL,LENGTH,LNUN,NT,
     7A1(60),A2(40),A3(60),A4(40),DLTT,KL10,NMAX1,WMAX,TIME
      REAL LENGTH
      LNUN=0
   20 LNUN=LNUN+1
      DPSILD=0.
      II=2
      MN=KL4
      IFL=ICMN
      JI=2
      IF (KL4-2) 10,11,10
```

```
   10 JI=3
   11 JFL=JLB
      IF (KL10-1) 990,12,990
   12 JI=3
      JFL=JLMN
  990 DO 22 J=JI,JFL
      DO 22 I=II,IFL
      DPSI=(0.5/(ZTSQ(J)+YTSQ(I)/B          ))*(PSI(I,J+1)*(ZTSQ(J)+0.5*
     1ZT2(J)*DLTZ)+PSI(I,J-1)*(ZTSQ(J)-0.5*ZT2(J)*DLTZ)+PSI(I+1,J)*
     2(YTSQ(I)          +YT2(I)*DLTY*0.5)*C*C+
     3PSI(I-1,J)*(YTSQ(I)          -YT2(I)*DLTY*0.5)*C*C-
     4DTZ2*VRT(I,J))       -PSI(I,J)
      PSI(I,J)=PSI(I,J)+BPSI*DPSI
      IF(ABS(DPSILD)-ABS(DPSI))    21,21,22
   21 DPSILD=DPSI
      ITS=I
      JTS=J
   22 CONTINUE
      II=IC
      IFL=ILMN
      GO TO (994,993),MN
  993 JI=J2+1
      JFL=J3-1
      MN=1
      GO TO 990
  994 IF (KL10-1) 23,15,23
   23 IF ((KL4)-(2)) 35,31014,35
31014 IFL=ICMN                                                    ))CASA>>
31013 DO 24 I=2,IFL
      PSI(I,1)=PSI(I,3)
   24 PSI(I,JL+1)=PSI(I,JL-1)
      RETURN
   15 IF (ABS(DPSILD)-DPSIM) 35,35,16
   16 IF (LNUN-NMAX1) 20,20,35
   35 RETURN
      END
```

```
// EXEC FORTRAN
      SUBROUTINE BOUND
      COMMON ICMN,IC,ICPL,ILMN,IL,ILPL,JLMN,JL,JLPL,KL0,KL1,KL3,KL4,KL5,
     1KL7,KL13,KL14,KL15,KL16,KL19,KL20,C,BPSI,BVRT,DPSIM,
     2RNN,DTZ2,DT2Y,Z(60),B,CWC,SVRCF,YTRN(40),Y(40),YSQ(40),
     3YT1(40),YTSQ(40),YT2(40),ZT1(60),ZTSQ(60),ZT2(60),
     4DIST(60),PSI(40,60),VRT(40,60),U(40,60),W(40,60),LN,
     5PSIMAX,ITV,JTV,DPSILD,DVRTLD,DLTY,DLTZ,JLB,ITS,JTS,
     6JLBPL,J2,JMMN,JM,JMPL,J3,P(40,60),EL,LENGTH,LNUN,NT,
     7A1(60),A2(40),A3(60),A4(40),DLTT,KL10,NMAX1,WMAX,TIME
      REAL LENGTH
      DIMENSION              A(60),BN(60),CN(60),D(60),X(60)
      VRT(IC,2)=-CWC*(PSI(IC,2) -PSI(ICMN,2) )*YTSQ(IC)
      VRT(1,2)=CWC*(PSI(2,2)-PSI(1,2)+DLTY*WMAX*LENGTH/(PSIMAX*YT1(1)))*
     1YTSQ(1)-YT2(1)*WMAX*LENGTH/(PSIMAX*YT1(1))
      DVRTLD=0.
      IVB=IC
      JI=2
      IF (KL10-1) 61,60,61
   60 JI=3
   61 DO 28 J=JI,JLB
      GO TO (998,997),KL4
  997 IVB=IC
      IF ((J)-(J2)) 998,31018,31018                                    ))CASA>>
31018 IF ((J)-(J3)) 31017,31017,998                                    ))CASA>>
31017 IVB=IL                                                           ))CASA>>
  998 VRTT=-CWC*(PSI(IVB,J)-PSI(IVB-1,J))*YTSQ(IVB)
      DVRT=VRTT-VRT(IVB,J)
      VRT(IVB,J)=VRTT
      IF(ABS(DVRTLD)-ABS(DVRT))    27,27,28
   27 DVRTLD=DVRT
      JTV=J
      ITV=IVB
   28 CONTINUE
      DO 50 J=JI,JLB
      VRTT=CWC*(PSI(2,J)-PSI(1,J)+DLTY*WMAX*LENGTH/(PSIMAX*YT1(1)))*
```

```
     1YTSQ(1)-YT2(1)*WMAX*LENGTH/(PSIMAX*YT1(1))
      DVRT=VRTT-VRT(1,J)
      VRT(1,J)=VRTT
      IF (ABS(DVRTLD)-ABS(DVRT))  53,53,50
   53 DVRTLD=DVRT
      JTV=J
      ITV=1
   50 CONTINUE
      IF (KL4-2) 93,31021,93                                          ))CASA>>
31021 JC=J2
      DO 40 I=IC,ILMN
   40 VRT(I,JC)=-2.0*ZTSQ(JC)*(PSI(I,JC)-PSI(I,JC+1))/DTZ2
      VRT(IC,JC)=VRT(IC,JC)-CWC*(PSI(IC,JC)-PSI(ICMN,JC))*YTSQ(IC)
      JC=J3
      DO 45 I=IC,ILMN
   45 VRT(I,JC)=-2.0*ZTSQ(JC)*(PSI(I,JC)-PSI(I,JC-1))/DTZ2
      VRT(IC,JC)=VRT(IC,JC)-CWC*(PSI(IC,JC)-PSI(ICMN,JC))*YTSQ(IC)
      GO TO 10
   93 DO 95 I=2,ICMN
      VRT(I,2) =-2.0*ZTSQ(2) *(PSI(I,2) -PSI(I,3))/DTZ2
   95 VRT(I,JL)=-2.0*ZTSQ(JL)*(PSI(I,JL)-PSI(I,JL-1))/DTZ2
      RETURN
   10 RETURN
      END
// EXEC FORTRAN
      SUBROUTINE VORTCT
      COMMON ICMN,IC,ICPL,ILMN,IL,ILPL,JLMN,JL,JLPL,KL0,KL1,KL3,KL4,KL5,
     1KL7,KL13,KL14,KL15,KL16,KL19,KL20,C,BPSI,BVRT,DPSIM,
     2RNN,DTZ2,DT2Y,Z(60),B,CWC,SVRCF,YTRN(40),Y(40),YSQ(40),
     3YT1(40),YTSQ(40),YT2(40),ZT1(60),ZTSQ(60),ZT2(60),
     4DIST(60),PSI(40,60),VRT(40,60),U(40,60),W(40,60),LN,
     5PSIMAX,ITV,JTV,DPSILD,DVRTLD,DLTY,DLTZ,JLB,ITS,JTS,
     6JLBPL,J2,JMMN,JM,JMPL,J3,P(40,60),EL,LENGTH,LNUN,NT,
     7A1(60),A2(40),A3(60),A4(40),DLTT,KL10,NMAX1,WMAX,TIME
      REAL LENGTH
      MN=KL4
```

```
      II=2
      IPL=ICPL
      IFL=ICMN
      JI=2
      IF (KL4-2) 10,11,10
   10 JI=3
   11 JFL=JLB
  990 DO 58 J=JI,JFL
      DO 58 IR=II,IFL
      I=IPL-IR
       BB=B*ZTSQ(J)/YTSQ(I)
      A=2.+2.*BB
      CR=(-YT2(I)+RNN*ZT1(J)*YT1(I)*
     1((PSI(I,J+1)-PSI(I,J-1))/(2.0*DLTZ))       )*DLTY/YTSQ(I)
      CZ=((-ZT2(J)-RNN*YT1(I)*ZT1(J)*((PSI(I+1,J)-PSI(I-1,J))/
     1(2.0*DLTY ))))*DLTY*DLTY/(YTSQ(I)*DLTZ)
      CALL COEF(CR,CZ,C1,C2,C3,C4,C5,C6,A,BVRT,CF)
      DVRT=((1.0  +C1*CR)*VRT(I+1,J)+(1.C  +C2*CR)*VRT(I-1,J)+(BB+C4*CZ)
     1*VRT(I,J+1)+(BB+C5*CZ)*VRT(I,J-1)
     2                  -(A+ C3*CR +  C6*CZ )*VRT(I,J))/CF
                     VRT(I,J)=VRT(I,J)+DVRT
      IF(ABS(DVRTLD)-ABS(DVRT))57,57,58                                  1PF02000
   57 DVRTLD=DVRT                                                        1PF02010
      ITV=I
      JTV=J
   58 CONTINUE                                                           1PF02020
      II=IC
      IFL=ILMN
      IPL=IL+ICMN
      GO TO (994,993),MN
  993 JI=J2+1
      JFL=J3-1
      MN=1
      GO TO 990
  994 IF (KL4-2) 85,75,85
   75 DO 70 I=2,ICMN
```

```
      VRT(I,1)=VRT(I,3)
   70 VRT(I,JL+1)=VRT(I,JL-1)
   85 RETURN
      END
// EXEC FORTRAN
      SUBROUTINE COEF(CR,CZ,C1,C2,C3,C4,C5,C6,A,B2,CF)
      IF (CR) 71,71,72
   71 C1=-1.C
      C2=0.0
      GO TO 73
   72 C1=0.0
      C2=1.0
   73 IF (CZ) 74,74,75
   74 C4=-1.0
      C5=0.0
      GO TO 76
   75 C4=0.0
      C5=1.0
   76 C3=C1+C2
      C6=C4+C5
   77 CF=A/B2+(C1+2.0*C2)*CR+(2.0*C4+C5)*CZ
      RETURN
      END
// EXEC FORTRAN
      SUBROUTINE ADI
      COMMON ICMN,IC,ICPL,ILMN,IL,ILPL,JLMN,JL,JLPL,KL0,KL1,KL3,KL4,KL5,
     1KL7,KL13,KL14,KL15,KL16,KL19,KL20,C,BPSI,BVRT,DPSIM,
     2RNN,DTZ2,DT2Y,Z(60),B,CWC,SVRCF,YTRN(40),Y(40),YSQ(40),
     3YT1(40),YTSQ(40),YT2(40),ZT1(60),ZTSQ(60),ZT2(60),
     4DIST(60),PSI(40,60),VRT(40,60),U(40,60),W(40,60),LN,
     5PSIMAX,ITV,JTV,DPSILD,DVRTLD,DLTY,DLTZ,JLB,ITS,JTS,
     6JLBPL,J2,JMMN,JM,JMPL,J3,P(40,60),HL,LENGTH,LNUN,NT,
     7A1(60),A2(40),A3(60),A4(40),DLTT,KL10,NMAX1,WMAX,TIME
      REAL LENGTH
      DIMENSION VRTN(40,60),A(60),BN(60),CN(60),D(60),X(60)
C
```

```
C      SWEEP IN I DIRECTION
C
       C2=1.0/DT2Y
       DO 20 I=2,ILMN
       GO TO (10,5),KL4
     5 IF (I-ICMN) 10,10,6
     6 JI=J2
       JFL=J3
       JFI=JFL-JI+1
       GO TO 11
    10 JI=2
       JFL=JL
       JFI=JLMN
    11 A(1)=0.0
       BN(1)=1.0
       CN(1)=0.0
       D(1)=VRT(I,JI)
       A(JFI)=0.0
       BN(JFI)=1.0
       CN(JFI)=0.0
       D(JFI)=VRT(I,JFL)
       JFIFL=JFI-1
       J=JI
       DO 15 JJ=2,JFIFL
       J=J+1
       C1=ZTSQ(J)/DTZ2
       C3= (RNN*ZT1(J)*(PSI(I+1,J)-PSI(I-1,J))/(2.0*DLTY)+ZT2(J))/
      1(2.0*DLTZ)
       C4=(-RNN*(PSI(I,J+1)-PSI(I,J-1))/(2.0*DLTZ))/DLTY
       A(JJ)=C1-C3
       BN(JJ)=-2.0*C1-2.0*RNN/DLTT
       CN(JJ)=C1+C3
    15 D(JJ)=-A(JJ)*VRT(I,J-1)-CN(JJ)*VRT(I,J+1)-(CWC+C4)*VRT(I+1,J)-
      1(CWC-C4)*VRT(I-1,J)+VRT(I,J)*(2.0*C1+2.0*CWC-2.0*RNN/DLTT)
       IF (NT-1) 16,14,16
    14 DO 50 JJ=2,JFIFL
```

```
   50 D(JJ)=0.0
   16 CALL SOLVE(A,BN,CN,C,X,JFI)
      J=JI-1
      DC 17 JJ=1,JFI
      J=J+1
   17 VRTN(I,J)=X(JJ)
   20 CONTINUE
C
C     SWEEP IN J DIRECTION
C
      DO 40 J=3,JLMN
      IFL=IL
      GO TO (30,25),KL4
   25 IF (J-J2) 27,27,26
   26 IF (J-J3) 30,27,27
   27 IFL=IC
   30 A(1)=0.0
      BN(1)=1.0
      CN(1)=0.0
      D(1)=VRT(1,J)
      D(IFL)=VRT(IFL,J)
      A(IFL)=0.0
      BN(IFL)=1.0
      CN(IFL)=0.0
      IFLMN=IFL-1
      DO 35  I=2,IFLMN
      C4=(-RNN*(PSI(I,J+1)-PSI(I,J-1))/(2.0*DLTZ))/DLTY
      A(I)=C2-C4/2.0
      BN(I)=-CWC-2.0*RNN/DLTT
      CN(I)=C2+C4/2.0
   35 D(I)=A(I)*VRT(I-1,J)+CN(I)*VRT(I+1,J)-CWC*VRT(I,J)-2.0*RNN*
     1VRTN(I,J)/DLTT
      IF (NT-1) 36,34,36
   34 DO 60 I=2,IFLMN
   60 D(I)=-2.0*RNN*VRTN(I,J)/DLTT
   36 CALL SOLVE(A,BN,CN,D,X,IFL)
```

```
      DO 37 I=1,IFL
   37 VRTN(I,J) =X(I)
   40 CONTINUE
      DO 45 I=2,ILMN
      DO 45 J=3,JLB
   45 VRT(I,J)=VRTN(I,J)
      RETURN
      END
// EXEC FORTRAN
      SUBROUTINE SOLVE(A,B,C,D,X,N)
      DIMENSION A(60),B(60),C(60),D(60),X(60)                                  */
      C(1)=C(1)/B(1)
      DO 5 I=2,N
      B(I)=B(I)-A(I)*C(I-1)
    5 C(I)=C(I)/B(I)
      D(1)=D(1)/B(1)
      DO 10 I=2,N
   10 D(I)=(D(I)-A(I)*D(I-1))/B(I)
      X(N)=D(N)
      NN=N-1
      DO 15 II=1,NN
      I=N-II
   15 X(I)=D(I)-C(I)*X(I+1)
      RETURN
      END
// EXEC FORTRAN
      SUBROUTINE CHRT
      COMMON ICMN,IC,ICPL,ILMN,IL,ILPL,JLMN,JL,JLPL,KL0,KL1,KL3,KL4,KL5,
     1KL7,KL13,KL14,KL15,KL16,KL19,KL20,C,BPSI,BVRT,DPSIM,
     2RNN,DTZ2,DT2Y,Z(60),B,CWC,SVRCF,YTRN(40),Y(40),YSQ(40),
     3YT1(40),YTSQ(40),YT2(40),ZT1(60),ZTSQ(60),ZT2(60),
     4DIST(60),PSI(40,60),VRT(40,60),U(40,60),W(40,60),LN,
     5PSIMAX,ITV,JTV,DPSILD,DVRTLD,DLTY,DLTZ,JLB,ITS,JTS,
     6JLBPL,J2,JMMN,JM,JMPL,J3,P(40,60),HL,LENGTH,LNUN,NT,
     7A1(60),A2(40),A3(60),A4(40),DLTT,KL10,NMAX1,WMAX,TIME
      REAL LENGTH
```

```
      MN=KL4
      II=2
      IFL=ICMN
      JI=2
      IF (KL4-2) 10,11,10
   10 JI=3
   11 JFL=JLB
  990 DO 20 J=JI,JFL
      DO 20 I=II,IFL
      W(I,J)=        -YT1(I)*(PSI(I+1,J)-PSI(I-1,J))/(2.0*DLTY)
   20 U(I,J)=          ZT1(J)*(PSI(I,J+1)-PSI(I,J-1))/(2.0*DLTZ)
      II=IC
      IFL=ILMN
      GO TO (994,993),MN
  993 JI=J2+1
      JFL=J3-1
      MN=1
      GO TO 990
  994 IF ((KL14)-(1)) 41,31033,41                                    ))CASA>>
31033 DO 35 J=1,JL
   35 DIST(J)=DIST(J)*LENGTH
      DO 40 I=1,IL
      Y(I)=Y(I)*LENGTH
      DO 40 J=1,JL
      U(I,J)=U(I,J)*PSIMAX/LENGTH
   40 W(I,J)=W(I,J)*PSIMAX/LENGTH
      KL5=1
      WRITE(3,190)
  190 FORMAT(1H1,51X,27HRESULTS IN DIMENSIONAL FORM,//)
   41 CONTINUE
      IF ((KL14)-(1)) 31035,31034,31035                              ))CASA>>
31035 WRITE(3,195)                                                   ))CASA>>
31034 CONTINUE
  195 FORMAT(1H1,50X,30HRESULTS IN NONDIMENSIONAL FORM,//)
C     IF KL3=6 WRITE PSI, VRT,U AND W ON UNIT 10
C     IF KL3=7 DO BOTH OF ABOVE
```

```
      IF (KL3-6) 601, 602, 601
  601 IF (KL3-7) 603, 602, 603
  602 REWIND 10
      WRITE (10)      (( PSI(I,J),I=1,IL), J=1,JL),
     1            (( VRT(I,J),I=1,IL), J=1,JL) ,
     2            ((   W(I,J),I=1,IL), J=1,JL),
     3            ((   U(I,J),I=1,IL), J=1,JL),TIME
      REWIND 10
  603 CONTINUE
      ILI1=1
      ILI2=6
   42 IF ((ILI2)-(IL)) 31036,31036,31037                          ))CASA>>
31037 ILI2=IL                                                     ))CASA>>
31036 ILI2D=ILI2
      WRITE(3,200) (Y(I),I=ILI1,ILI2)
  200 FORMAT(24X,4HY(I),1X,1P6E17.7)
      WRITE(3,205)
  205 FORMAT(//,3X,1HJ,6X,7HDIST(J),/)
      DO 45 J=1,JL
      ILI2=ILI2D
      GO TO (999,997),KL4
  997 IF (J-J2) 1001,1000,1000
 1000 IF (J-J3) 999,999,1001
 1001 IF (ILI1-IC) 31038,31038,44
31038 IF (ILI2-IC) 999,999,1002
 1002 ILI2=IC
  999 WRITE(3,210) J,DIST(J),(U(I,J),I=ILI1,ILI2)
  210 FORMAT(2X,I2,1PE16.6,6X,1HU,2X,6E17.7)
      WRITE(3,220) (W(I,J),I=ILI1,ILI2)
  220 FORMAT(26X,1HW,2X,1P6E17.7)
      IF ((KL5)-(1)) 31044,43,31044                              ))CASA>>
31044 WRITE(3,225) (PSI(I,J),I=ILI1,ILI2)
  225 FORMAT(25X,3HPSI,1X,1P6E17.7)
      WRITE (3,230) (VRT(I,J),I=ILI1,ILI2)
  230 FORMAT(25X,3HVRT,1X,1P6E17.7)
   43 WRITE (3,235)
```

```
  235 FORMAT(/)
      GO TO 45
   44 WRITE (3,250)
  250 FORMAT(/////)
   45 CONTINUE
      IF ((ILI2D)-(IL)) 31045,46,46                                    ))CASA>>
31045 ILI1=ILI2D+1
      ILI2=ILI2D+6
      WRITE (3,237)
  237 FORMAT(1H1)
      GO TO 42
   46 CONTINUE
      WRITE (3,240) PSIMAX
  240 FORMAT(//,4X,7HPSIMAX=1PE17.7)
  420 IF ((KL3)-(1)) 31047,31046,31047
31047 RETURN                                                           ))CASA>>
31046 ILI1=1
      ILI2=5
  342 IF ((ILI2)-(IL)) 31048,31048,31049                               ))CASA>>
31049 ILI2=IL                                                          ))CASA>>
31048 DO 345 J=1,JL
      WRITE(2,310) J,(U(I,J),I=ILI1,ILI2)
  310 FORMAT(1X,I2,1X,1P5E15.7)
      WRITE(2,315) (W(I,J),I=ILI1,ILI2)
  315 FORMAT(4X,1P5E15.7)
  345 CONTINUE
      IF ((ILI2)-(IL)) 31050,346,346                                   ))CASA>>
31050 ILI1=ILI2+1
      ILI2=ILI2+5
      GO TO 342
  346 CONTINUE
      RETURN                                                           1PF03990
      END                                                              1PF04000
```

REFERENCES

1. Kistler, A.L. and Tan, F.C. "Some Properties of Turbulent Separated Flows", The Physics of Fluid Supplement, (1967), 165-173.

2. Batchelor, G., Journal of Fluid Mechanics, 1 (1956), 388.

3. Burggraf, O.R., "Analytical and Numerical Studies of the Structure of Steady Separated Flows", Journal of Fluid Mechanics, 24 (1966), 113-151.

4. Mills, R.D., "On the Closed Motion of a Fluid in a Square Cavity", Journal of the Royal Aeronautical Society, 69 (1965), 116-120.

5. Mills, R.D., "Numerical Solutions of the Viscous Flow Equations for a Class of Closed Flows", Journal of the Royal Aeronautical Society, 69 (1965), 714-718.

6. Kawaguti, M., "Numerical Solution of the Navier-Stokes Equations for the Flow in a Two-Dimensional Cavity", Journal of Physical Society of Japan, 16 (1961), 2307-2315.

7. Pan, F. and Acrivos, A., "Steady Flows in Rectangular Cavities", Journal of Fluid Mechanics, 28 (1967), 643-655.

8. Moffatt, H.K., "Viscous and Resistive Eddies Near a Sharp Corner", Journal of Fluid Mechanics, 18 (1964), 1-18.

9. O'Brien, V., "Periodic Boundary Layer Flows Over a Flat Plate Part III: With Disturbance Bars", TG-944, Applied Physics Laboratory, The Johns Hopkins University, August 1967.

10. Brandt, A., "Solutions of Equations in Hydrodynamics and Magnetohydrodynamics", Weizmann Institute of Science, Israel (1964).

11. Bird, R.B., Stewart, W.E. and Lightfoot, E.H., Transport Phenomena, John Wiley and Sons, Inc., New York, 1960.

12. Aziz, K., "A Numerical Study of Cellular Convection", Ph.D. Thesis, Rice University (1966).

13. Lavan, Z. and Fejer, A.A., "Investigations of Swirling Flows in Ducts", ARL 66-0083, Aerospace Research Laboratories, USAF, Wright-Patterson Air Force Base, Ohio, May 1966.

14. Douglas (Jr.), J., "Alternating Direction Methods for Three Space Variables", Numerische Mathematik, 4 (February 1962), 41-63.

15. Wilkes, J.O., "The Finite Difference Computation of Natural Convection in an Enclosed Rectangular Cavity", Ph.D. Thesis, University of Michigan (1963).

NASA-Langley, 1968 —— 12 E-4573

"The aeronautical and space activities of the United States shall be conducted so as to contribute . . . to the expansion of human knowledge of phenomena in the atmosphere and space. The Administration shall provide for the widest practicable and appropriate dissemination of information concerning its activities and the results thereof."

—NATIONAL AERONAUTICS AND SPACE ACT OF 1958

NASA SCIENTIFIC AND TECHNICAL PUBLICATIONS

TECHNICAL REPORTS: Scientific and technical information considered important, complete, and a lasting contribution to existing knowledge.

TECHNICAL NOTES: Information less broad in scope but nevertheless of importance as a contribution to existing knowledge.

TECHNICAL MEMORANDUMS: Information receiving limited distribution because of preliminary data, security classification, or other reasons.

CONTRACTOR REPORTS: Scientific and technical information generated under a NASA contract or grant and considered an important contribution to existing knowledge.

TECHNICAL TRANSLATIONS: Information published in a foreign language considered to merit NASA distribution in English.

SPECIAL PUBLICATIONS: Information derived from or of value to NASA activities. Publications include conference proceedings, monographs, data compilations, handbooks, sourcebooks, and special bibliographies.

TECHNOLOGY UTILIZATION PUBLICATIONS: Information on technology used by NASA that may be of particular interest in commercial and other non-aerospace applications. Publications include Tech Briefs, Technology Utilization Reports and Notes, and Technology Surveys.

Details on the availability of these publications may be obtained from:

SCIENTIFIC AND TECHNICAL INFORMATION DIVISION

NATIONAL AERONAUTICS AND SPACE ADMINISTRATION

Washington, D.C. 20546